As for electrophysiological characteristics, AA, atrio–His, and His–ventricular intervals showed no significant differences among the 3 groups. VA was more frequently induced from the RVOT than from the RVA (57 [70%] vs 24 [30%], respectively).

Subsequent cardiac events during follow-up

We recommended all patients with prior VF episode, group SD patients, and group T patients with prior syncope to undergo an ICD implantation. For asymptomatic group T patients, and group N patients without prior VF, ICD implantation was performed only for those who wanted it after informed consent. Forty-one of the 45 group SD patients (91%), 25 of the 36 group T patients (69%), and 13 of the 27 group N patients (48%) underwent an ICD implantation.

There were no deaths during 82 ± 48 months of follow-up; 24 patients had VF events. All these 24 patients had undergone ICD implantation, and VF was documented on the recordings of the ICD. No patients without ICD experienced any syncope. There were no significant differences in the follow-up period among the 3 groups (group SD 83 ± 50 months, group T 81 ± 44, and group N 80 ± 49; P = .96). Significantly more VF episodes occurred in group SD (16 of 45 [36%]) than in group T (3 of 36 [8%]) and in group N (5 of 27 [19%]) (P = .012).

Figure 1 shows the results of the Kaplan–Meier analysis of subsequent cardiac events. As previously reported, induction of VA was not associated with subsequent cardiac events (Figure 1A, log-rank, P = .78). When we focused on the numbers of extrastimuli, group SD had a significantly higher risk of subsequent cardiac events than did group T (log-rank, P = .004), but there were no significant differences in the subsequent cardiac event rate between group SD and group N and between group T and group N (Figure 1B). Among 82 patients without prior VF episode, VA induction with up to 2 extrastimuli was a significant risk factor of subsequent cardiac events (Figure 1C, log-rank, P = .003).

In 81 patients with induced VA, the site of induction (the RVA or the RVOT) and the coupling interval of extrastimuli at the time of VA induction (<200 ms or ≥200 ms) were not associated with subsequent cardiac events (Figures 2A and 2B, log-rank, P = .57 and .52, respectively). The cardiac event rate was associated with the number of extrastimuli, not with the site of induction and the coupling interval (Figures 3A and 3B).

As for 42 asymptomatic patients, 2 of the 17 patients in group SD experienced subsequent VF episodes, whereas none of the 14 patients in group T and 11 in group N experienced subsequent cardiac events. Although the number of patients was small, group SD showed a significantly higher cardiac event rate than did group T and group N (log-rank, P = .046).

Predictors of long-term prognosis

The results of Cox regression analysis are shown in Table 3. In univariate Cox regression, history of VF, VA induced with up to 2 extrastimuli, incidence of spontaneous coved-type ST segment, and Late potential were significant predictors of subsequent cardiac events. Multivariate Cox re-

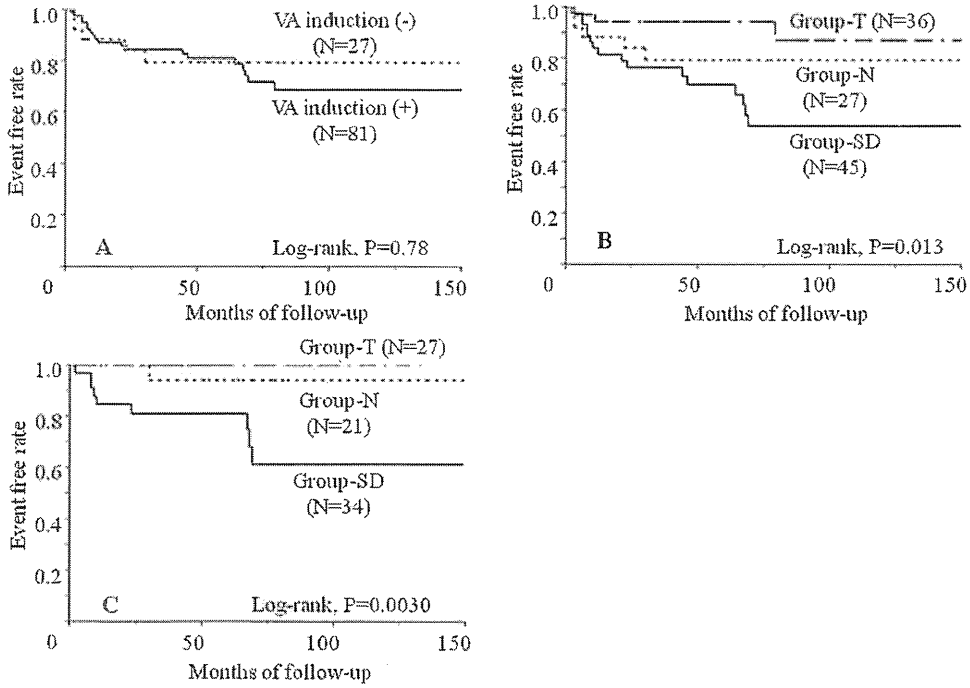

Figure 1 Kaplan–Meier curves of subsequent cardiac events during follow-up. Kaplan–Meier curves of cardiac events (**A**) depending on the overall inducibility of ventricular arrhythmias (VFs and polymorphic ventricular tachycardia >15 successive beats) by up to triple extrastimuli, (**B**) in the 3 groups, and (**C**) in the population of patients without history of VF depending on the 3 groups. Although the overall inducibility was not associated with subsequent cardiac events, inducibility by up to 2 extrastimuli had significant predictive values for the occurrence of subsequent cardiac events. Group SD had a significantly higher cardiac event rate than did group T. In the population of patients without previous VF, inducibility by up to 2 extrastimuli was strongly associated with subsequent cardiac events.

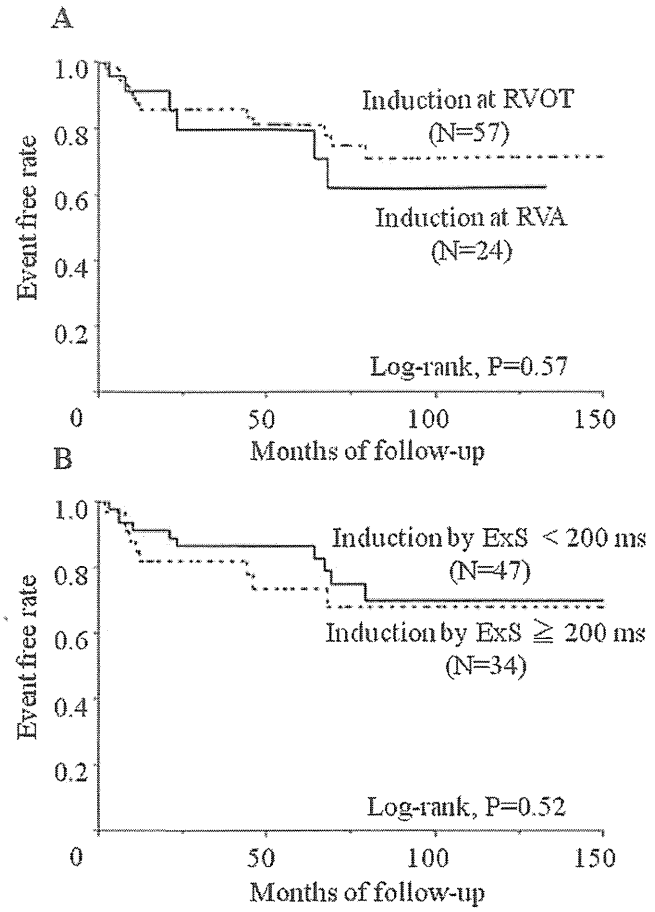

Figure 2 Kaplan–Meier curves of subsequent cardiac events during follow-up. Kaplan–Meier curves of cardiac events (**A**) depending on the induction site and (**B**) the minimum coupling interval of extrastimuli at the time of induction. Neither the site of induction, the right ventricular outflow tract or the right ventricular apex, nor the minimum coupling interval, longer or shorter than 200 ms, was associated with subsequent cardiac events.

gression demonstrated that the only predictive index was VA induction with up to 2 extrastimuli except for history of VF. Neither VA induction from the RVA nor the coupling interval of extrastimuli <200 ms at the time of VA induction was a predictor of subsequent cardiac events.

Discussion

The major findings of the present study were the following: (1) induction of VA by triple extrastimuli was not associated with a higher incidence of subsequent VF, (2) patients with VA induced by up to 2 extrastimuli had significantly more frequent VF episodes during 7 years of follow-up, (3) neither the site of VA induction (the RVA or the RVOT) nor the coupling interval of VA induction (<200 ms or ≥200 ms) was associated with the incidence of subsequent cardiac events.

We evaluated the prognostic role of VA induction by PES and found that the number of extrastimuli that induced VA was prognostic for patients with Brugada type 1 ECG.

Clinical significance of PES in patients with BrS

Conflicting data have been reported from several registries as to the prognostic value of PES in patients with BrS.[4,6,7] Brugada et al reported that PES was a good predictor of arrhythmic events. Meanwhile, Priori et al and Probst et al argued that it was not a useful index. Meta-analysis data indicated that PES was not useful for predicting subsequent cardiac events, and the published ACC/AHA/ESC guidelines referred to PES as a class IIb indication in asymptomatic patients with BrS for risk stratification.[11–13] However, there were several limitations for each registry such as the different PES protocols.[14] Moreover, these conflicting data may be related to the specific inclusion criteria of each registry. Recently, Giustetto et al[9] reported that PES protocol up to 2 extrastimuli with ventricular effective refractory period was useful in risk stratification in patients with BrS. This Italian study agrees with our result that VA induction with up to 2 extrastimuli could help predict subsequent cardiac events if a consistent PES protocol is used. The present study also demonstrated that a PES protocol with up to 3 extrastimuli was not useful for risk stratification in patients with BrS. We presume that this result in part explains why several registries reported conflicting data.

Patients without VA induction, especially patients with history of VF, had subsequent arrhythmic events in the present study (5 of 27 [19%]). In this respect, the present study differs from the Italian study. We can cite 2 contributing factors. First, our follow-up period was nearly 7 years, which was much longer than that of the Italian study. Second, we adopted only 1 basic cycle length, whereas Giustetto et al adopted 2 basic cycle lengths; hence, it is possible that we could not induce VA in some patients.

Underlying mechanism

Arrhythmogenicity in patients with BrS is possibly associated with both repolarization and depolarization abnormal-

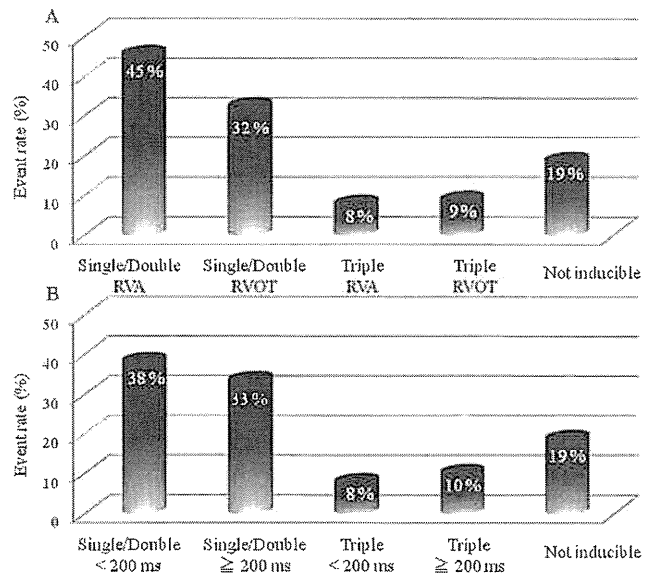

Figure 3 Incidence of subsequent cardiac events according to the number of extrastimuli, the site of induction, and the minimum coupling interval at the time of induction. Incidence of cardiac events (**A**) according to the number of extrastimuli and the site of induction and (**B**) the number of extrastimuli and the minimum coupling interval. The patients whose ventricular arrhythmias were induced by up to 2 extrastimuli had a higher incidence of cardiac events in both categories.

Table 3 Predictive factors of subsequent cardiac events

	Univariate analysis		Multivariate analysis	
	Hazard ratio	*P* value	Hazard ratio	*P* value
Hx of VF	4.59 (2.05–10.7)	<.001	3.47 (1.50–8.27)	.004
VA induced with double extrastimuli	3.21 (1.41–7.92)	.005	3.03 (1.26–8.00)	.013
Spontaneous coved-type ST segment	3.20 (1.28–9.65)	.011	1.77 (0.67–5.56)	.26
Late potential	2.72 (1.02–9.40)	.046	1.77 (0.60–5.98)	.34
SCN5A mutation	2.92 (0.96–7.33)	.057	1.66 (0.47–4.63)	.40
VA induction at the RVA	1.29 (0.47–3.07)	.60		
VA induced with CI < 200 ms	0.86 (0.37–1.91)	.71		
VA induced by PES	1.21 (0.48–3.64)	.71		
Family Hx of sudden death under age 45	1.18 (0.39–2.95)	.74		

CI = coupling interval; Hx = history; PES = programmed electrical stimulation; RVA = right ventricular apex; VA = ventricular arrhythmia; VF = ventricular fibrillation. Parentheses represent 95% confidence interval.

ities. In the present study, patients with induced VA had longer LAS40 (49±17 vs 41±13; $P = .042$) and smaller RMS40 (15±10 vs 20±13; $P = 0.034$) than did noninduced patients, which may reflect depolarization abnormality and is concordant with our previous report.[15]

There have been several reports regarding depolarization abnormalities in BrS such as *SCN5A* mutation or fragmented QRS.[16–18] By using an experimental model, Aiba et al[19] showed that depolarization abnormalities played a significant role in VF maintenance. Thus, if PES results reflect depolarization abnormality, we could evaluate how easily VF continues through PES. The initiation of VF is thought to be due to phase 2 reentry-induced premature beats (repolarization abnormality).[19,20] It could be difficult to evaluate repolarization abnormality through PES, and this is why PES in BrS cannot completely predict subsequent cardiac events.

Clinical implication

According to the ACC/AHA/ESC guidelines, patients with BrS with spontaneous ST-segment elevation and syncope are a class IIa indication for ICD implantation.[13] However, some patients with BrS experience neurally mediated syncope, as previously reported, which should be distinguished from syncope of unknown origin.[21] Therefore, only the history of syncope could lead to unnecessary use of ICD. We showed that PES of up to 2 extrastimuli can predict subsequent events of patients with prior syncope, demonstrating the possibility that PES could help reduce the unnecessary use of ICD in those patients (Figure 1C).

Meta-analysis studies of patients with BrS could not identify a significant role of PES for predicting subsequent arrhythmic events.[11,12] However, many registries included in their meta-analysis adopted PES protocol of up to 3 extrastimuli. Triple extrastimuli could induce VA even in normal individuals and exaggerate nonspecific depolarization abnormality leading to induction of nonspecific VA. This suggests that VA induction by triple extrastimuli may be highly unnatural, resulting in false-positive VA induction.

ACC/AHA/ESC guidelines have not yet delineated an appropriate PES protocol in detail, such as the number of extrastimuli. We showed that single extrastimulus or double extrastimuli are adequate for PES for patients with BrS. Although the number of patients was small, VA induction with up to 2 extrastimuli was associated with subsequent arrhythmic events even in asymptomatic patients. Positive and negative predictive values according to PES protocols are shown in Table 4. Based on our criteria that VA induction was considered positive when VF or PVT with more than 15 successive beats was elicited, a protocol of up to 2 extrastimuli showed that the positive predictive value (PPV) was 36% and the negative predictive value (NPV) was 87%. On the other hand, a protocol of up to 3 extrastimuli showed that PPV was 23% and NPV was 81%. Even when we consider only VF as an induction criterion, both PPV and NPV were higher with up to 2 extrastimuli (Table 4). Based on our data, protocols up to 2 extrastimuli were sufficient for PES in patients with BrS. In the subgroup of 82 patients without prior VF or aborted cardiac arrest, VF occurred in 9 of the 34 patients with VA induced by up to 2 extrastimuli. No VF occurred in 27 patients with VA induced by triple extrastimuli, and only 1 of the 21 noninducible patients experienced VF. The PPV of PES protocol up to 2 extrastimuli was 26%, but the NPV was high at 98%. However, a low PPV of PES can cause unnecessary use of ICD implantation, especially for asymptomatic patients. We still need to make a decision based on several indices combined, as Delise et al[22] have recently reported.

Table 4 Positive and negative predictive values according to protocols of PES

Protocols	PPV	NPV
VF and NSPVT >15 successive beats		
PES with up to 2 ExS	16/45 (36%)	55/63 (87%)
PES with up to 3 ExS	19/81 (23%)	22/27 (81%)
Only VF		
PES with up to 2 ExS	13/40 (33%)	57/68 (84%)
PES with up to 3 ExS	16/71 (23%)	29/37 (78%)

ExS = extrastimuli; NPV = negative predictive value; NSPVT = nonsustained polymorphic ventricular tachycardia; PES = programmed electrical stimulation; PPV = positive predictive value; VF = ventricular fibrillation.

Study limitations

This study has several limitations. First, this was a retrospective study. However, we believe that our data have validity because this was not an interventional study but an observational study, and moreover, the follow-up periods of the 3 groups were not significantly different. Second, this study consisted of a small population of 108 patients, insufficient to fully evaluate the prognosis of patients with BrS. Further study with a larger number of patients with BrS and with consistent protocol of PES will be required to draw a firm conclusion on the importance of the number of extrastimuli. If each registry does not have a large enough number of patients, a meta-analysis that can compare the numbers of extrastimuli could validate the significance of PES. Third, we could have underestimated the cardiac event rate because the end point of the patients without ICD was based on symptoms (syncope); thus, asymptomatic cardiac events during sleep could be missed. Fourth, we adopted only 500 ms as a basic cycle length, and so VA could not be induced in some patients in the present study because this was shorter than in other studies that employed more than 2 basic cycle lengths. However, VA was induced in 75% and VF was induced in 68% of the patients. This induction rate was comparable to that in other registries; this suggests that a single basic cycle length of 500 ms is enough to induce VA. We did not deliver extrastimuli coupled with intervals shorter than 180 ms. Therefore, we could not assess the significance of delivering extrastimuli with intervals shorter than 180 ms. However, extra stimulus with shorter intervals may exaggerate nonspecific depolarization abnormality, leading to induction of nonspecific VA. This issue needs to be addressed. Fifth, the incidence of *SCN5A* mutation was relatively low at 11%, even though we searched the entire coding sequence of *SCN5A*. As previously pointed out, the incidence of *SCN5A* in Japan is lower than in Western countries, and so this study agrees with previous data.[23,24] Finally, there were 46 patients (7 with prior VF, 21 with prior syncope, and 18 asymptomatic) with drug-induced type 1 ECG, which can be misdiagnosed as BrS because of its false-positive ECG morphology. However, the percentage of these patients was lower than that in the FINGER study, and we confirmed the obvious coved ST elevation induced by sodium-channel–blocker test in patients with type 2 and type 3 ECG.

Conclusion

The number of extrastimuli in PES that induced ventricular arrhythmias served as a prognostic indicator for patients with type 1 Brugada ECG. The site of induction and the coupling interval of extrastimuli at the time of VF induction were not prognostic indicators of patients with BrS. Our data suggest that PES in patients with type 1 Brugada ECG should employ up to 2 extrastimuli, rather than 3.

References

1. Brugada P, Brugada J. Right bundle branch block, persistent ST segment elevation and sudden cardiac death: a distinct clinical and electrocardiographic syndrome: a multicenter report. J Am Coll Cardiol 1992;20:1391–1396.
2. Kamakura S, Ohe T, Nakazawa K, et al, for the Brugada Syndrome Investigators in Japan. Long-term prognosis of probands with Brugada-pattern ST-elevation in leads V1–V3. Circ Arrhythm Electrophysiol 2009;2:495–503.
3. Brugada J, Brugada R, Antzelevitch C, et al. Long-term follow-up of individuals with the electrocardiographic pattern of right bundle-branch block and ST-segment elevation in precordial leads V1 to V3. Circulation 2002; 105:73–78.
4. Priori SG, Napolitano C, Gasparini M, et al. Natural history of Brugada syndrome: insights for risk stratification and management. Circulation 2002;105: 1342–1347.
5. Ikeda T, Takami M, Sugi K, Mizusawa Y, Sakurada H, Yoshino H. Noninvasive risk stratification of subjects with a Brugada-type electrocardiogram and no history of cardiac arrest. Ann Noninvasive Electrocardiol 2005;10: 396–403.
6. Makimoto H, Nakagawa E, Takaki H, et al. Augmented ST-segment elevation during recovery from exercise predicts cardiac events in patients with Brugada syndrome. J Am Coll Cardiol 2010;56:1576–1584.
7. Probst V, Veltmann C, Eckardt L, et al. Long-term prognosis of patients diagnosed with Brugada syndrome: results from the FINGER Brugada syndrome registry. Circulation 2010;121:635–643.
8. Brugada P, Brugada R, Mont L, Rivero M, Geelen P, Brugada J. Natural history of Brugada syndrome: the prognostic value of programmed electrical stimulation of the heart. J Cardiovasc Electrophysiol 2003;14:455–457.
9. Giustetto C, Drago S, Demarchi PG, et al. Risk stratification of the patients with Brugada type electrocardiogram: a community-based prospective study. Europace 2009;11:507–513.
10. Antzelevitch C, Brugada P, Borggrefe M, et al. Brugada syndrome: report of the second consensus conference: endorsed by the Heart Rhythm Society and the European Heart Rhythm Association. Circulation 2005;111:659–670.
11. Gehi AK, Duong TD, Metz LD, Gomes JA, Mehta D. Risk stratification of individuals with the Brugada electrocardiogram: a meta-analysis. J Cardiovasc Electrophysiol 2006;17:577–583.
12. Paul M, Gerss J, Schulze-Bahr E, et al. Role of programmed ventricular stimulation in patients with Brugada syndrome: a meta-analysis of worldwide published data. Eur Heart J 2007;28:2126–2133.
13. Zipes DP, Camm AJ, Borggrefe M, et al. ACC/AHA/ESC2006 guidelines for management of patients with ventricular arrhythmias and the prevention of sudden cardiac death. Circulation 2006;114:e385–e484.
14. Gasparini M, Priori SG, Mantica M, et al. Programmed electrical stimulation in Brugada syndrome: how reproducible are the results? J Cardiovasc Electrophysiol 2002;13:880–887.
15. Kanda M, Shimizu W, Matsuo K, et al. Electrophysiologic characteristics and implications of induced ventricular fibrillation in symptomatic patients with Brugada syndrome. J Am Coll Cardiol 2002;39:1799–1805.
16. Smits JP, Eckardt L, Probst V, et al. Genotype–phenotype relationship in Brugada syndrome: electrocardiographic features differentiate SCN5A-related patients from non-SCN5A-related patients. J Am Coll Cardiol 2002; 40:350–356.
17. Yokokawa M, Noda T, Okamura H, et al. Comparison of long-term follow-up of electrocardiographic features in Brugada syndrome between the SCN5A-positive probands and the SCN5A-negative probands. Am J Cardiol 2007;100: 649–655.
18. Morita H, Kusano KF, Miura D, et al. Fragmented QRS as a marker of conduction abnormality and a predictor of prognosis of Brugada syndrome. Circulation 2008;118:1697–1704.
19. Aiba T, Shimizu W, Hidaka I, et al. Cellular basis for trigger and maintenance of ventricular fibrillation in the Brugada syndrome model: high-resolution optical mapping study. J Am Coll Cardiol 2006;47:2074–2085.
20. Yan GX, Antzelevitch C. Cellular basis for the Brugada syndrome and other mechanisms of arrhythmogenesis associated with ST-segment elevation. Circulation 1999;100:1660–1666.
21. Yokokawa M, Okamura H, Noda T, et al. Neurally mediated syncope as a cause of syncope in patients with Brugada electrocardiogram. J Cardiovasc Electrophysiol 2010;21:186–192.
22. Delise P, Allocca G, Marras E, et al. Risk stratification in individuals with the Brugada type 1 ECG pattern without previous cardiac arrest: usefulness of a combined clinical and electrophysiologic approach. Eur Heart J 2011;32:169–176.
23. Hiraoka M. Inherited arrhythmic disorders in Japan. J Cardiovasc Electrophysiol 2003;14:431–434.
24. Kapplinger JD, Tester DJ, Alders M, et al. An international compendium of mutations in the SCN5A-encoded cardiac sodium channel in patients referred for Brugada syndrome genetic testing. Heart Rhythm 2010;7:33–46.

Effect of sodium-channel blockade on early repolarization in inferior/lateral leads in patients with idiopathic ventricular fibrillation and Brugada syndrome

Hiro Kawata, MD,*† Takashi Noda, MD, PhD,* Yuko Yamada, MD,* Hideo Okamura, MD,* Kazuhiro Satomi, MD, PhD,* Takeshi Aiba, MD, PhD,* Hiroshi Takaki, MD,* Naohiko Aihara, MD,* Mitsuaki Isobe, MD, PhD,† Shiro Kamakura, MD, PhD,* Wataru Shimizu, MD, PhD*

*From the *Division of Arrhythmia and Electrophysiology, Department of Cardiovascular Medicine, National Cerebral and Cardiovascular Center, Suita, Osaka, Japan; †Department of Cardiovascular Medicine, Tokyo Medical and Dental University, Tokyo, Japan.*

BACKGROUND A high incidence of early repolarization (ER) pattern in the inferolateral leads has been reported in patients with idiopathic ventricular fibrillation (IVF). Brugada syndrome (BS) is characterized by J-point or ST-segment elevation in the right precordial leads and ventricular fibrillation, and some patients with BS also have ER in the inferolateral leads.

OBJECTIVE To compare the clinical characteristics and effects of sodium-channel blockade on ER between IVF patients with ER (early repolarization syndrome [ERS]) and BS patients with or without ER.

METHODS Fourteen patients with ERS and 21 patients with BS were included in this study. ER was defined as an elevation of at least 0.1 mV from baseline in the QRS-T junction in the inferoro-lateral leads. Provocative tests with sodium-channel blockers were conducted in all patients with ERS to distinguish ERS from BS.

RESULTS In the ERS group, all patients were male and most patients experienced ventricular fibrillation during sleep or low activity (79%). ER was attenuated by sodium-channel blockers in most patients with ERS (13/14, 93%) and BS (5/5, 100%), whereas ST-segment elevation was augmented in the right precordial leads in the BS group. The rates of positive late potentials were significantly higher in the BS group (60%) than in the ERS group (7%) ($P < .01$).

CONCLUSIONS Some similarities were observed between ERS and BS, including gender, arrhythmia triggers, and response of ER to sodium-channel blockers. Unlike the ST segment in the right precordial leads in BS, ER was attenuated in patients with both ERS and BS, suggesting a differential mechanism between ER in the inferolateral leads and ST elevation in the right precordial leads.

KEYWORDS Early repolarization; J wave; Idiopathic ventricular fibrillation; Brugada syndrome; Sudden death; Sodium-channel blocker

ABBREVIATIONS **BS** = Brugada syndrome; **ECG** = electrocardiogram; **ER** = early repolarization; **ERS** = early repolarization syndrome; **IVF** = idiopathic ventricular fibrillation; **LPs** = late potentials; **QTc** = corrected QT interval; **SAECG** = signal-averaged electrocardiogram; **SCD** = sudden cardiac death; **VF** = ventricular fibrillation; **VT** = ventricular tachycardia

(Heart Rhythm 2012;9:77–83)

Introduction

Early repolarization (ER) pattern is often found in the general population and has been considered a benign electrocardiographic finding. Its prevalence has been estimated to be between 1% and 5% of healthy adults.[1–4] Idiopathic ventricular fibrillation (IVF) presenting prominent ST-segment elevation in the inferior leads has been considered as a variant of Brugada syndrome (BS).[5,6] BS[7] is characterized by ST-segment elevation in the right precordial leads V1 to V3 and is considered to have a high propensity toward sudden cardiac death (SCD).[8,9] Recently, several reports have suggested the association of IVF with ER in the inferior and/or lateral lead in the electrocardiogram (ECG).[3,10–14] ER is reported to be found more frequently among patients with IVF than among healthy control subjects.[10,15] However, little is known about the clinical and electrocardiographic characteristics and the pharmacological response of ER in patients with IVF and BS associated with ER and their different re-

Dr Shimizu was supported in part by the Research Grant for the Cardiovascular Diseases (21C-8, 22-4-7, H23-114) from the Ministry of Health, Labour and Welfare, Japan, and Grant-in-Aid for Scientific Research on Innovative Areas (22136011). This article was presented in part at the American Heart Association 2010, Chicago, Illinois, November 13–17, 2010, and published as an abstract (Circulation 2010;122:A14948).

Address for reprints and correspondence: Dr Wataru Shimizu, MD, PhD, Division of Arrhythmia and Electrophysiology, Department of Cardiovascular Medicine, National Cerebral and Cardiovascular Center, 5-7-1 Fujishiro-dai, Suita, Osaka 565-8565, Japan. E-mail address: wshimizu@hsp.ncvc.go.jp.

1547-5271/$ -see front matter doi:10.1016/j.hrthm.2011.08.017

sponse from that of ST elevation in the right precordial leads in patients with BS. The present study aimed to investigate the similarities and differences between IVF with ER (early repolarization syndrome [ERS]) and BS with or without ER.

Methods

Patient characteristics

Among 38 patients with IVF, admitted to the National Cerebral and Cardiovascular Center between 1994 and 2009, ER in the inferior and/or lateral ECG leads was recorded in 14 patients (37%). These 14 patients were included in this study as an ERS group (all males, aged 27–64 years, mean age 44.7 ± 13.6 years). Twenty-one patients with BS with a history of ventricular fibrillation (VF) or aborted SCD were also included in this study. According to the published guidelines,[16,17] patients were diagnosed as suffering from IVF if they had no structural heart disease confirmed by noninvasive studies (physical examination, ECG, exercise stress test, echocardiogram, and cardiac magnetic resonance imaging or computed tomography) and invasive studies (coronary angiography and left ventricular cineangiography). Long QT syndrome (corrected QT [QTc] interval ≥440 millisecond), short QT syndrome (QTc interval <340 millisecond), and BS were also excluded to diagnose a patient as suffering from IVF. To exclude BS, all subjects in the ERS group were proven to be negative with a pharmacological challenge with pilsicainide.[8,18]

The BS group consisted of 21 patients (19 males, aged 20–64 years, mean age 39.7 ± 12.6 years) with an episode of documented VF or aborted SCD. Eleven had a spontaneous type 1 ECG, and in the remaining, it was induced by a sodium-channel blocker. Ethical approval of the present study was obtained from the Institutional Review Committee of the National Cerebral and Cardiovascular Center.

Electrocardiography

All available conventional ECGs (25 mm/s, 10 mm/mV) were investigated in the search for ER. ER was defined as an elevation of at least 1 mm (0.1 mV) in the J point (QRS–ST junction) in at least 2 leads (Figure 1), either as QRS slurring (smooth transition from QRS to the ST segment) or as notching (a positive J deflection inscribed on the S wave).[10] The inferior (II, III, and aVF) and lateral (I, aVL, and V4–V6) leads were evaluated. To exclude BS, no J-point elevation must exist in the right precordial leads (V1–V3).

All ECGs were interpreted blindly by 2 independent cardiologists (H.K., W.S.). The following parameters were assessed in lead II, which include P-wave duration and PQ and RR intervals. QRS duration and QT interval were assessed in leads II and V5. The QTc interval was calculated using Bazett's method. The amplitude of ER was assessed in the inferior leads (II, III, and aVF), the lateral leads (I, aVL, and V4–V6), or both, and the maximum ER amplitude was measured. We selected leads II and V5 as representative of inferior and lateral leads for the analysis of ER amplitude.

BS was diagnosed when a type 1 coved-type ST-segment elevation (≥0.2 mV at J point) was observed in >1 of the right precordial leads (V1–V3) in the presence or absence of

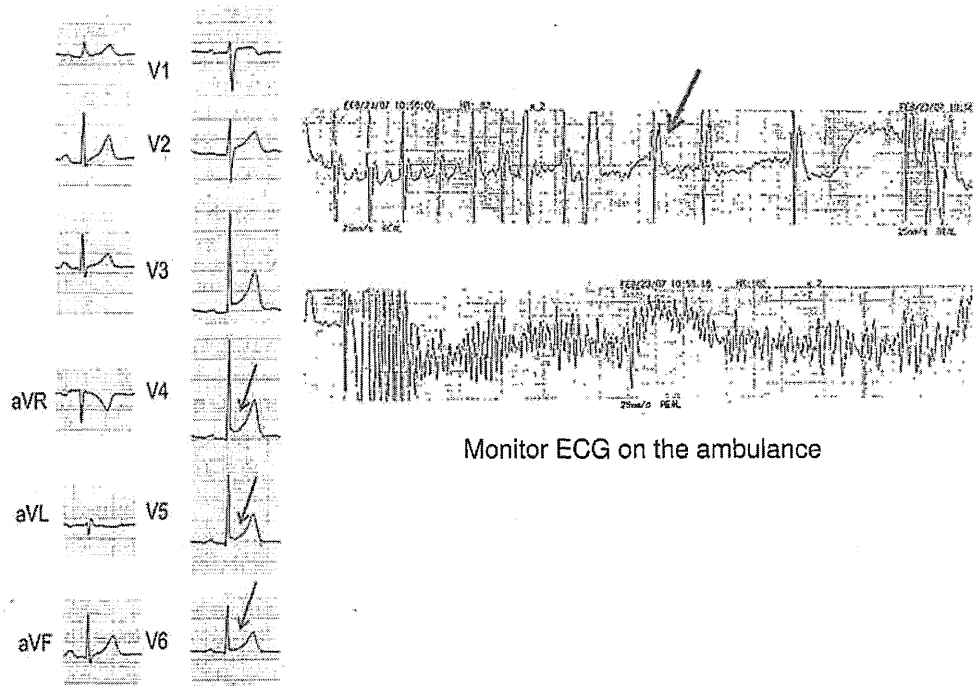

Figure 1 **A:** Twelve-lead ECG in a patient with early repolarization syndrome. ER (arrow) was seen in the lateral leads (V4–V6) under baseline conditions. **B:** Monitor ECG recorded during the arrhythmic periods in the same patient showed a consistent increase in the amplitude of ER, followed by initiation of ventricular fibrillation. ECG, electrocardiogram; ER, early repolarization.

a sodium-channel blocker in conjunction with documented VF or polymorphic ventricular tachycardia (VT).

Drug challenge test

The drug challenge test was performed with intravenous pilsicainide (1 mg/kg, maximum 50 mg, 5 mg/min) or flecainide (2 mg/kg, maximum 100 mg, 10 mg/min). The test result was considered positive if a type 1 Brugada ECG appeared in >1 right precordial lead (V1–V3). Once again, we excluded all patients with IVF but without sodium-channel blocker challenge test from our study to clarify the diagnosis of ERS.

Late potentials

Late potentials (LPs) were analyzed by using a signal-averaged electrocardiogram (SAECG) system (Arrhythmia Research Technology 1200EPX, Milwaukee, WI). Three parameters were assessed by using a computer algorithm: (1) total filtered QRS duration (f-QRS), (2) duration of low-amplitude signals <40 μV of the filtered QRS complex (LAS_{40}), and (3) root-mean-square voltage of the terminal 40 millisecond of the filtered QRS complexes (RMS_{40}). LPs were considered positive when at least 2 of the 3 parameters were abnormal: f-QRS >120 millisecond, LAS_{40} >38 millisecond, and RMS_{40} <18 μV.

Statistical analysis

Continuous variables were expressed as mean value ± SD. A comparison between the 2 groups was performed with Student's t test for paired data. Categorical variables were compared with Fisher's exact test. A P value of <.05 was regarded as being significant.

Results

Clinical and electrocardiographic characteristics

In the BS group, 9 of the 21 patients (43%) with BS showed ER in the inferior and/or lateral leads. A comparison of the clinical and electrocardiographic characteristics of the 14 ERS group patients, 21 BS group patients, and 9 BS patients with ER is shown in Table 1. The average age of 9 BS patients with ER was lower than that of the ERS group. Except for that, no significant differences were observed in baseline clinical characteristics with respect to age, gender, family history of SCD, and activity at the time of cardiac arrest. The number of premature ventricular complexes during 24-hour Holter ECG was not different between the 2 groups.

Regarding SAECG parameters, the values of f-QRSd, LAS_{40}, and RMS_{40} in 14 ERS group patients were 97.8 ± 8.1 millisecond, 29.8 ± 5.2 μV, and 50.0 ± 24.2 millisecond, respectively. The corresponding values in 21 BS group patients were 119.8 ± 17.3 millisecond, 47.0 ± 19.2 μV, and 17.8 ± 13.4 millisecond, respectively. All these parameters were significantly different between the 2 groups. LPs were positive in 1 of the 14 patients (7%) in the ERS group and in 12 of the 20 patients (60%) in the BS group. The rate of positive LPs was significantly higher in the BS group than in the ERS group (P <.01). We also compared the SAECG parameters and the rate of positive LPs between 14 ERS group patients and 9 BS patients with ER. The tendency was similar to the comparison between 14 ERS group patients and 21 BS group patients; however, there were no significant differences in the LAS_{40} and rate of LPs because of the small number of BS patients with ER.

Table 1 Clinical and electrocardiographic characteristics in the early repolarization syndrome group, the Brugada syndrome group, and the Brugada syndrome with ER group

	Group			P value	
	ERS (n = 14)	BS (n = 21)	BS with ER (n = 9)	ERS vs BS	ERS vs BS with ER
Clinical characteristics					
Age (y), mean ± SD	44.7 ± 13.6	39.7 ± 12.6	33.3 ± 10.3	NS	.045
Male gender, n/N	14/14	19/21	7/9	NS	NS
Family history of sudden cardiac death, n/N (%)	0/14 (0%)	1/21 (5%)	1/9 (11%)	NS	NS
Activity at the time of cardiac arrest, n (%)					
Sleep	3 (21%)	9 (42%)	5 (55%)	NS	NS
Rest	8 (57%)	10 (48%)	3 (33%)	NS	NS
Others	3 (21%)	2 (10%)	1 (11%)	NS	NS
Electrocardiographic characteristics					
Presence of ER, n/N (%)	14/14 (100%)	9/21 (43%)	9/9 (100%)	<.01	NS
Holter ECG, PVC in 24 h, mean ± SD	49.4 ± 169.3	1.9 ± 4.2	2.3 ± 4.4	NS	NS
Signal-averaged electrocardiography, mean ± SD					
f-QRSd (ms)	97.8 ± 8.1	119.8 ± 17.3	111.6 ± 11.5	<.0001	<.01
LAS_{40} (μV)	29.8 ± 5.2	47.0 ± 19.2	33.8 ± 14.5	<.01	NS
RMS_{40} (ms)	50.0 ± 24.2	17.8 ± 13.4	23.4 ± 14.2	<.0001	<.01
Abnormal SAECG, n/N (%)	1/14 (7%)	12/20 (60%)	4/9 (44%)	<.01	NS

Percentages may not total 100 because of rounding.

BS, Brugada syndrome; ECG, electrocardiogram; ER, early repolarization; ERS, early repolarization syndrome; f-QRSd, filtered QRS duration; LAS_{40}, duration of low-amplitude signals <40 μV of QRS in the terminal filtered QRS complex; NS, not significant; PVC, premature ventricular contraction; RMS_{40}, root-mean-square voltage of the terminal 40 millisecond of the filtered QRS complex; SAECG, signal-averaged ECG.

Table 2 Baseline electrocardiographic parameters and their changes after administration of a sodium-channel blocker in the early repolarization syndrome group, the Brugada syndrome group, and the Brugada syndrome with ER group

	Mean ± SD			*P* value	
	ERS (n = 14)	BS (n = 12)	BS with ER (n = 5)	ERS vs BS	ERS vs BS with ER
RR II (ms)	951 ± 116	930 ± 116	1024 ± 46	NS	NS
ΔRR II (ms)	−71 ± 41	−12 ± 17	−32 ± 62	<.05	NS
P II (ms)	104 ± 19	110 ± 16	112 ± 13	NS	NS
ΔP II (ms)	10 ± 9	21 ± 13	24 ± 16	<.05	<.05
PQ II (ms)	179 ± 34	191 ± 33	178 ± 28	NS	NS
ΔPQ II (ms)	30 ± 9	28 ± 14	38 ± 8	NS	NS
QRS II (ms)	90 ± 13	97 ± 18	90 ± 20	NS	NS
ΔQRS II (ms)	10 ± 10	23 ± 21	14 ± 21	NS	NS
QRS V5 (ms)	84 ± 8	91 ± 19	82 ± 21	NS	NS
ΔQRS V5 (ms)	13 ± 8	29 ± 18	28 ± 8	<.05	<.01
QT II (ms)	377 ± 19	370 ± 14	374 ± 15	NS	NS
ΔQT II (ms)	10 ± 14	28 ± 18	16 ± 5	NS	NS
QTcII (ms)	388 ± 20	385 ± 24	370 ± 13	NS	NS
ΔQTcII (ms)	10 ± 14	29 ± 18	16 ± 5	<.05	NS
QT V5 (ms)	376 ± 26	372 ± 17	376 ± 15	NS	NS
ΔQT V5 (ms)	6 ± 18	38 ± 23	14 ± 11	<.01	NS
QTcV5 (ms)	387 ± 23	387 ± 24	372 ± 12	NS	NS
ΔQTcV5 (ms)	7 ± 19	40 ± 25	14 ± 11	<.01	NS

BS = Brugada syndrome; ER = early repolarization; ERS = early repolarization syndrome; P = P-wave duration; PQ = PQ interval; QRS = QRS duration; QT = QT interval; QTc = corrected QT interval; RR = RR interval.

Sodium-channel blocker infusion test

The sodium-channel blocker infusion test was performed in 12 of the 21 patients with BS, and the test result was positive in all 12 patients. We compared the pharmacological responses of several ECG parameters to a sodium-channel blocker between 14 patients with ERS and 12 patients with BS (Table 2). There were no significant differences in the baseline ECG parameters, including RR interval, P-wave duration, PQ interval, QRS duration, and QT interval in any leads. Shortening of RR (ΔRR II) was significantly larger in the ERS group. Prolongation of P-wave duration (ΔP II), QRS duration (ΔQRS V5), and QTc interval (ΔQTc II, ΔQTc V5) was significantly larger in the BS group compared with that in the ERS group.

Among 9 BS patients with ER, the sodium-channel blocker test was performed in 5 patients. We also compared the ECG parameters between 14 ERS group patients and 5 BS patients with ER (Table 2). Prolongation of P-wave duration (ΔP II) and QRS duration (ΔQRS V5) was significantly larger in the BS with ER group compared with that in the ERS group.

The ER amplitude and its responses to sodium-channel blockers between 14 ERS group patients and 5 BS patients with ER are shown in Table 3. In the ERS group, ER was observed in the inferior leads (II, III, and aVF) in 9 patients, in the lateral leads (I, aVL, and V4–V6) in 8 patients, and in both the inferior and lateral leads in 3 patients. In the 9 BS patients with ER, ER was observed in the inferior leads in 6 patients, in the lateral leads in 8 patients, and in both the inferior and lateral leads in 5 patients. The baseline maximum ER amplitude among the inferolateral leads (pre-ER max) in the BS group tended to be higher than in the ERS group (0.244 ± 0.082 vs 0.162 ± 0.069 mV; $P = .057$). The baseline ER amplitude in the inferior lead (pre-ER II) was significantly higher in the BS group than in the ERS group (0.236 ± 0.081 vs 0.120 ± 0.033 mV; $P < .05$). After administration of a sodium-channel blocker, the ER ampli-

Table 3 Amplitude of ER in leads II and V5 before and after the administration of a sodium-channel blocker test in the early repolarization syndrome group and the Brugada syndrome with ER group

Maximum amplitude of ER in any inferolateral leads (mV)	Mean ± SD		
	ERS (n = 14)	BS with ER (n = 5)	*P* value
Pre-ER max	0.162 ± 0.069	0.244 ± 0.082	NS
Post-ER max	0.081 ± 0.061*	0.124 ± 0.096*	NS
ΔER	0.080 ± 0.067	0.120 ± 0.058	NS
Amplitude of ER in the inferior lead (II) (mV)	**ERS (n = 9)**	**BS (n = 5)**	
Pre-ER II	0.120 ± 0.033	0.236 ± 0.081	<.05
Post-ER II	0.091 ± 0.054*	0.104 ± 0.086*	NS
ΔER II	0.028 ± 0.051	0.132 ± 0.068	<.05
Amplitude of ER in the lateral lead (V5) (mV)	**ERS (n = 8)**	**BS (n = 5)**	
Pre-ER V5	0.116 ± 0.032	0.215 ± 0.092	NS
Post-ER V5	0.010 ± 0.022*	0.137 ± 0.094*	NS
ΔER V5	0.106 ± 0.026	0.077 ± 0.071	NS

BS = Brugada syndrome; ER = early repolarization; ERS = early repolarization syndrome; max = maximum; pre = before sodium-channel blocker test; post = after sodium-channel blocker infusion; Δ = change.
*$P < .05$ vs pre.

tude was attenuated in all 5 patients with BS (100%) and in 13 of 14 patients with ERS (93%). ER attenuation was occasionally associated with the appearance of an S wave in both the groups (Figure 2). Therefore, the maximum ER amplitude (ER max), ER amplitude in the inferior lead (ER II), and ER amplitude in the lateral lead (ER V5) all were significantly decreased after the administration of sodium-channel blockers ($P < .05$). Figure 3 illustrates the differential response to sodium-channel blockers between the ER in the inferolateral leads and the J point and ST segment in the right precordial leads in a patient with BS. The coved-type (type 1) ECG was unmasked and the J point in the right precordial leads (V1–V3) was augmented by the sodium-channel blocker, whereas the ER amplitude in the inferolateral leads (II, III, aVF, and V4–V6) was attenuated (Figure 3B).

Discussion

The ER pattern in the inferior and/or lateral leads had been considered benign, and it is often found in healthy young individuals. Recently, several reports have attracted increasing attention to the association of IVF with ER in the inferior and/or lateral leads.[5,10,19–21] Haissaguerre et al[10] reported that ER was more frequently recognized in patients with IVF than in control subjects and that there was a higher incidence of recurrent VF in case subjects with ER than in those without. Rosso et al[15] also reported that ER was found more frequently among patients with IVF than among healthy control subjects. On the other hand, BS is also characterized by a high incidence of VF without structural heart disease. The Brugada Consensus Report proposed that type 1 coved-type ST-segment elevation in the right precordial lead (V1–V3) in the absence or presence of a sodium-channel blocker was required to diagnose BS.[22] Considering this diagnostic criterion, the sodium-channel blocker challenging test is essential to exclude BS. In order to investigate pure ERS, the sodium-channel blocker challenging test should be performed before the diagnosis of ERS. Unlike previous studies,[10,15] we conducted the sodium-channel blocker challenging test in all 14 patients with ERS to exclude BS in the present study.

Intravenous administration of sodium-channel blockers has been used to unmask the Brugada ECG pattern in patients with BS.[23] On the other hand, in most patients associated with ER in both the ERS group and the BS group of the present study, the administration of a sodium-channel blocker induced the attenuation or disappearance of the ER and appearance of an S wave. Attenuation of the ER in the inferolateral leads appears to be due largely to a slowing of the transmural conduction so that inscription of the ER occurs later on the descending limb of the QRS in both the ERS group and the BS group. The S-wave appearance in the inferolateral leads is also probably due to the conduction delay induced by sodium-channel blockers. This may indicate the differential mechanism between Brugada-type ST elevation in the right precordial lead of BS and ER in the inferolateral leads in both groups.

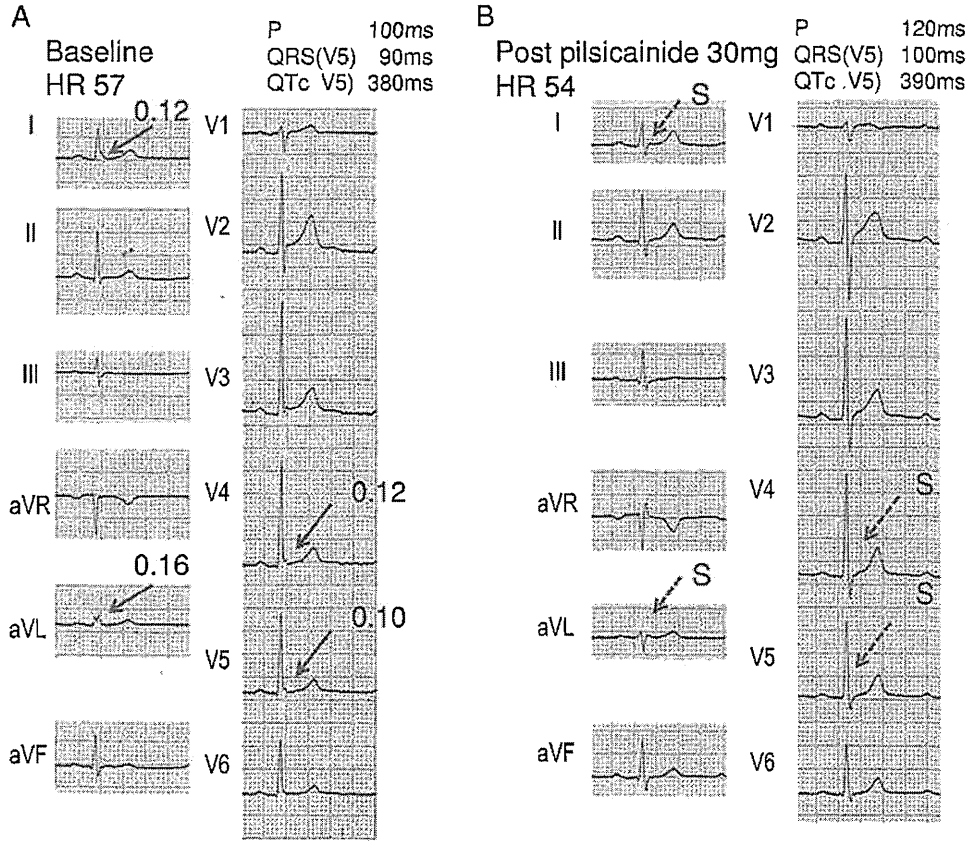

Figure 2 Twelve-lead ECGs in a patient with early repolarization syndrome under baseline conditions (**A**) and after pilsicainide administration (**B**). ER was seen in the lateral leads (I, aVL, and V4–V5) under baseline conditions (**A**, arrows). Intravenous administration of 30 mg of pilsicainide induced attenuation of ER and appearance of an S wave in the lateral leads (dashed arrows). Numbers above the arrows indicate the amplitude of ER. ECG, electrocardiogram; ER, early repolarization; S, S wave.

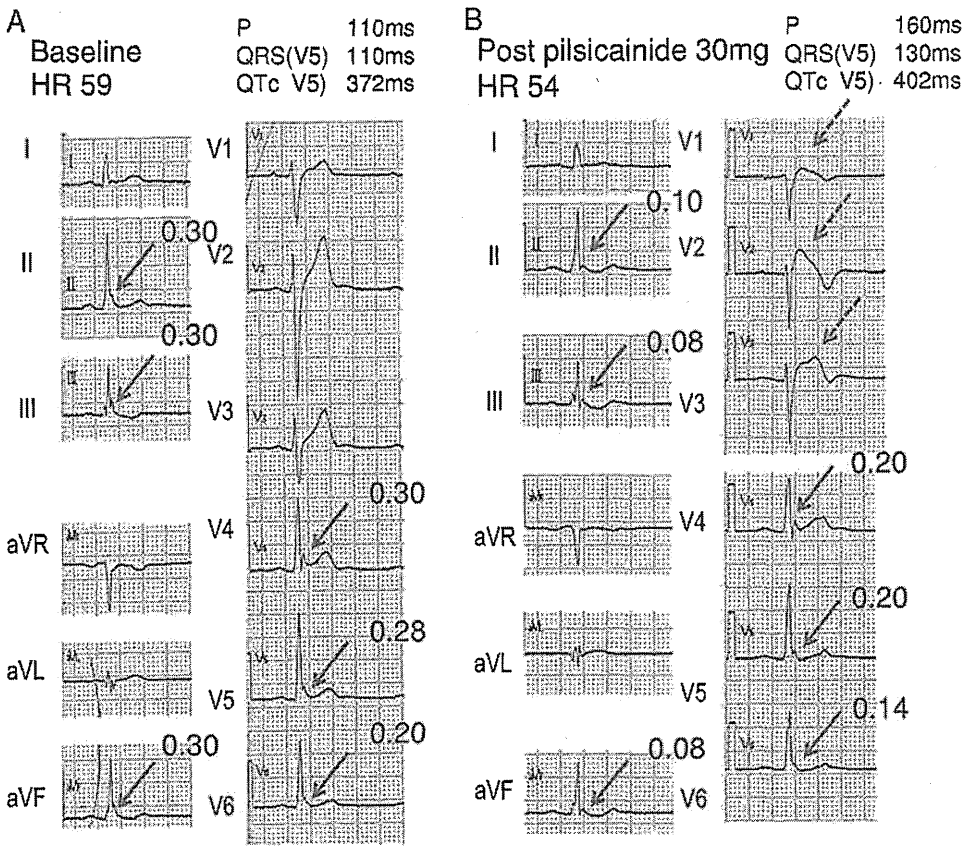

Figure 3 Twelve-lead ECGs in a patient with Brugada syndrome under baseline conditions (**A**) and after pilsicainide administration (**B**). ER was seen in the inferior (II, III, and aVF) and lateral (V4–V6) leads under baseline conditions (**A**, arrows). Intravenous administration of 30 mg of pilsicainide unmasked coved-type Brugada ECG and remarkably augmented the J point and ST segment in the right precordial leads (V1–V3) (**B**, dashed arrows), while ER was attenuated in the inferior and lateral leads (**B**, arrows). Numbers above the arrows indicate the amplitude of ER. ECG, electrocardiogram; ER, early repolarization.

Antzelevitch and Gan-Xin[24] have proposed a new concept that an outward shift in repolarizing current due to a decrease in sodium- or calcium-channel currents or an increase in outward currents such as a transient outward potassium current (I_{to}) can give rise to J-wave syndromes, which includes BS, ERS, hypothermia, and acute ischemia–induced VF. A prominent and pathological J wave, a slow upright deflection between the end of the QRS complex and the early portion of the ST segment, has been reported to be seen often in hypothermia.[25] However, the terms J-wave syndromes and ERS have not been properly defined.[26]

In some patients with BS of this study, type 1 Brugada ECG was unmasked by a sodium- channel blocker in the right precordial lead, while ER was attenuated in the inferolateral leads (Figure 3). Once again, this finding suggested the differential mechanism between Brugada-type ECG in the right precordial lead and ER in the inferolateral leads.

Moreover, as with a previous report,[27] the BS group showed significantly larger prolongation of P-wave duration, QRS duration, and QTc interval compared with the ERS group after a sodium-channel blocker infusion. Basic electrophysiology including animal or mathematical models must play an important role in determining whether the cellular mechanism of ST-segment elevation in the right precordial leads in BS and that of ER in the inferolateral leads in both ERS and BS differ or not.

Our study showed clinical characteristics of ERS to be similar to those of BS, including adult onset, male preponderance, cardiac events occurred at rest or during sleep, and rare ventricular arrhythmias on Holter ECG.[28,29] On the other hand, some apparent differences were found between the 2 groups, including LPs on the SAECG. All 3 parameters of the SAECG were significantly different between the 2 groups, and the positive rate of LPs was significantly lower in the ERS group than in the BS group. The rate of LPs has been previously reported to be high in BS.[30] On the other hand, Haissaguerre et al[10] also reported a relatively low rate (11%) of LPs in patients with ERS. LPs are reported to be not only highly prevalent in BS but also independent predictors of VT/VF inducibility.[27,31–33] LPs are also considered to be linked to VF inducibility during electrophysiological study and ventricular conduction delay during VF induction in patients with BS[28,34] as well as in patients with VT/VF associated with organic heart diseases. The ST-segment elevation in the right precordial leads and arrhythmogenicity in BS can be explained by both repolarization and depolarization abnormalities in right ventricular outflow.[9,35] The presence of LPs can be caused by conduction delay (depolarization abnormality) in the ventricle including the right ventricular outflow tract. On the other hand, from the experimental studies, LPs are explained on the basis of repolarization abnormality (late phase 2 upstroke and concealed phase 2 reentry) in the right ventricular outflow tract.[36] In the present study, the lower prevalence of LPs in the ERS group may indicate a differential substrate for VF in patients with ERS compared with that in patients with BS.

Conclusions

ER can be seen in some patients with IVF and in a subgroup of subjects with BS. Clinical similarities among them exist, including age, gender, and arrhythmia triggers. Response to sodium-channel blockade on ER in the inferolateral leads is the same in both groups: a consistent diminution in ER amplitude. This effect contrasts with the ST-segment elevation that is always observed in the right precordial leads in BS, thus arguing for different pathophysiological mechanisms.

References

1. Klatsky AL, Oehm R, Cooper RA, Udaltsova N, Armstrong MA. The early repolarization normal variant electrocardiogram: correlates and consequences. Am J Med 2003;115:171–177.
2. Mehta M, Jain AC, Mehta A. Early repolarization. Clin Cardiol 1999;22:59–65.
3. Gussak I, Antzelevitch C. Early repolarization syndrome: clinical characteristics and possible cellular and ionic mechanisms. J Electrocardiol 2000;33:299–309.
4. Tikkanen JT, Anttonen O, Junttila MJ, et al. Long-term outcome associated with early repolarization on electrocardiography. N Engl J Med 2009;361:2529–2537.
5. Kalla H, Yan GX, Marinchak R. Ventricular fibrillation in a patient with prominent J (Osborn) waves and ST segment elevation in the inferior electrocardiographic leads: a Brugada syndrome variant? J Cardiovasc Electrophysiol 2000;11:95–98.
6. Takagi M, Aihara N, Takaki H, et al. Clinical characteristics of patients with spontaneous or inducible ventricular fibrillation without apparent heart disease presenting with J wave and ST segment elevation in inferior leads. J Cardiovasc Electrophysiol 2000;11:844–848.
7. Brugada P, Brugada J. Right bundle branch block, persistent ST segment elevation and sudden cardiac death: a distinct clinical and electrocardiographic syndrome. A multicenter report. J Am Coll Cardiol 1992;20:1391–1396.
8. Antzelevitch C, Brugada P, Borggrefe M, et al. Brugada syndrome: report of the second consensus conference: endorsed by the Heart Rhythm Society and the European Heart Rhythm Association. Circulation 2005;111:659–670.
9. Shimizu W, Aiba T, Kamakura S. Mechanisms of disease: current understanding and future challenges in Brugada syndrome. Nat Clin Pract Cardiovasc Med 2005;2:408–414.
10. Haissaguerre M, Derval N, Sacher F, et al. Sudden cardiac arrest associated with early repolarization. N Engl J Med 2008;358:2016–2023.
11. Aizawa Y, Tamura M, Chinushi M, et al. Idiopathic ventricular fibrillation and bradycardia-dependent intraventricular block. Am Heart J 1993;126:1473–1474.
12. Ogawa M, Kumagai K, Yamanouchi Y, Saku K. Spontaneous onset of ventricular fibrillation in Brugada syndrome with J wave and ST-segment elevation in the inferior leads. Heart Rhythm 2005;2:97–99.
13. Potet F, Mabo P, Le Coq G, et al. Novel brugada SCN5A mutation leading to ST segment elevation in the inferior or the right precordial leads. J Cardiovasc Electrophysiol 2003;14:200–203.
14. Shinohara T, Takahashi N, Saikawa T, Yoshimatsu H. Characterization of J wave in a patient with idiopathic ventricular fibrillation. Heart Rhythm 2006;3:1082–1084.
15. Rosso R, Kogan E, Belhassen B, et al. J-point elevation in survivors of primary ventricular fibrillation and matched control subjects: incidence and clinical significance. J Am Coll Cardiol 2008;52:1231–1238.
16. Zipes DP, Wellens HJ. Sudden cardiac death. Circulation 1998;98:2334–2351.
17. Consensus Statement of the Joint Steering Committees of the Unexplained Cardiac Arrest Registry of Europe and of the Idiopathic Ventricular Fibrillation Registry of the United States. Survivors of out-of-hospital cardiac arrest with apparently normal heart: need for definition and standardized clinical evaluation. Circulation 1997;95:265–272.
18. Brugada R, Brugada J, Antzelevitch C, et al. Sodium channel blockers identify risk for sudden death in patients with ST-segment elevation and right bundle branch block but structurally normal hearts. Circulation 2000;101:510–515.
19. Sinner FM, Reinhard W, Müller M, et al. Association of early repolarization pattern on ECG with risk of cardiac and all-cause mortality: a population-based prospective cohort study (MONICA/KORA). PLoS Med 2010;7:e1000314.
20. Haruta D, Matsuo K, Tsuneto A, et al. Incidence and prognostic value of early repolarization pattern in the 12-lead electrocardiogram. Circ Arrhythm Electrophysiol 2011;123:2931–2937.
21. Noseworthy PA, Tikkanen JT, Porthan K, et al. The early repolarization pattern in the general population: clinical correlates and heritability. J Am Coll Cardiol 2011;31:2284–2289.
22. Wilde AAM, Antzelevitch C, Borggrefe M, et al. Proposed diagnostic criteria for the Brugada syndrome: consensus report. Circulation 2002;106:2514–2519.
23. Brugada J, Brugada P. Further characterization of the syndrome of right bundle branch block, ST segment elevation, and sudden cardiac death. J Cardiovasc Electrophysiol 1997;8:325–331.
24. Antzelevitch C, Gan-Xin Y. J wave syndromes. Heart rhythm 2010;7:549–558.
25. Surawicz B, Knilans T. Chou's Electrocardiography in Clinical Practice: Adult and Pediatric. 6th ed. Philadelphia: WB Saunders; 2008.
26. Surawicz B, Macfarlane PW. Inappropriate and confusing electrocardiographic terms: J-wave syndromes and early repolarization. J Am Coll Cardiol 2011;57:1584–1586.
27. Shimizu W, Antzelevitch C, Suyama K, et al. Effect of sodium channel blockers on ST segment, QRS duration, and corrected QT interval in patients with Brugada syndrome. J Cardiovasc Electrophysiol 2000;11:1320–1329.
28. Matsuo K, Kurita T, Inagaki M, et al. The circadian pattern of the development of ventricular fibrillation in patients with Brugada syndrome. Eur Heart J 1999;20:465–470.
29. Corrado D, Basso C, Buja G, Nava A, Rossi L, Thiene G. Right bundle branch block, right precordial ST-segment elevation, and sudden death in young people. Circulation 2001;103:710–717.
30. Ajiro Y, Hagiwara N, Kasanuki H. Assessment of markers for identifying patients at risk for life-threatening arrhythmic events in Brugada syndrome. J Cardiovasc Electrophysiol 2005;16:45–51.
31. Meregalli PG, Wilde AAM, Tan HL. Pathophysiological mechanisms of Brugada syndrome: depolarization disorder, repolarization disorder, or more? Cardiovasc Res 2005;67:367–378.
32. Nademanee K, Veerakul G, Nimmannit S, et al. Arrhythmogenic marker for the sudden unexplained death syndrome in Thai men. Circulation 1997;96:2595–2600.
33. Ikeda T, Sakurada H, Sakabe K, et al. Assessment of noninvasive markers in identifying patients at risk in the Brugada syndrome: insight into risk stratification. J Am Coll Cardiol 2001;37:1628–1634.
34. Kanda M, Shimizu W, Matsuo K, et al. Electrophysiologic characteristics and implications of induced ventricular fibrillation in symptomatic patients with Brugada syndrome. J Am Coll Cardiol 2002;39:1799–1805.
35. Yokokawa M, Noda T, Okamura H, et al. Comparison of long-term follow-up of electrocardiographic features in Brugada syndrome between the SCN5A-positive probands and the SCN5A-negative probands. Am J Cardiol 2007;100:649–655.
36. Wilde AAM, Postema PG, Di Diego JM, et al. The pathophysiological mechanism underlying Brugada syndrome: depolarization versus repolarization. J Mol Cell Cardiol 2010;49:543–553.

Abrupt Heart Rate Fallings in a Patient with Biventricular Pacing: Latent Risk for Exacerbation of Heart Failure

HIRO KAWATA, M.D.,* TAKASHI NODA, M.D.,* YUKO YAMADA, M.D.,* HIDEO OKAMURA, M.D.,* HIROYUKI NAKAJIMA, M.D.,† JUNJIRO KOBAYASHI, M.D.,† and SHIRO KAMAKURA, M.D.*

From the *Division of Cardiology, Department of Internal Medicine, National Cardiovascular Center, Suita, Japan; and †Department of Cardiovascular Surgery, National Cardiovascular Center, Suita, Japan

This case report describes abrupt heart rate fallings below the lower pacing rate limit in a patient with cardiac resynchronization therapy (CRT). Interrogated information including stored episodes or data regarding the lead did not show any device problems and only simultaneous intracardiac electrogram revealed the cause, T-wave oversensing during biventricular pacing. At this moment, CRT has become an established modality for patients with severe heart failure. However, bradycardia below the lower rate limit during biventricular pacing due to T-wave oversensing would exacerbate heart failure in patients with CRT. We should notice this latent risk and correct the malfunction immediately. (PACE 2012; 35:e55–e58)

T-wave oversensing, CRT, device malfunction

Introduction

Many studies have demonstrated that cardiac resynchronization therapy (CRT) is established modality for patients with severe heart failure.[1,2] Not only heart failure symptoms, but also the rate of mortality or hospitalization were improved by CRT. To respond to CRT, there are several factors. It is important to capture the ventricles consistently by biventricular pacing with appropriate heart rate and we should be well aware of CRT device malfunction.[3] Postpacing T-wave oversensing is one of pacing device malfunction and can cause inappropriate bradycardia.[4] This phenomenon appears only after pacing, so it cannot be stored as episodes on the device leading to be overlooked. Here, we report abrupt heart rate fallings below the lower pacing rate limit in a patient with CRT. Only simultaneous intracardiac electrogram (EGM) revealed the cause, which was T-wave oversensing during biventricular pacing.

Case Report

The patient was a 68-year-old man who underwent a valve replacement for aortic regurgitation complicated with left ventricular dysfunction. He developed atrioventricular block and received a pacemaker in 1994. Subsequently, he developed dyspnea on effort with New York Heart Association functional class III. On echocardiography, the left ventricule was markedly dilated and its function was severely impaired with a left ventricular ejection fraction of 24%. Both interventricular and intraventricular dyssynchrony were confirmed. He underwent removal of previous pacemaker and implantation of CRT device with defibrillator (CRT-D) (Concerto C174AWK, Medtronic Inc., Minneapolis, MN, USA). All procedures were performed successfully without any complication. Initially, the lower pacing rate limit was set at 70 beats per minute (bpm). He continued his hospitalization to adjust the medical therapy for heart failure and CRT-D. Twelve days after the implantation, his monitor electrocardiogram displayed abrupt heart rate fallings below the lower pacing rate limit (Fig. 1). Interrogated and checked information including the lead impedance or capture threshold did not reveal any device problem. There were no events that suggested noises due to the lead fracture or electromagnetic interference. Close monitoring was continued. Finally, we could get intracardiac EGM during abnormal bradycardia pacing simultaneously (Fig. 2). The intracardiac EGM showed T-wave oversensing during biventricular pacing. Time from BV (biventricular pacing spike) to TS (ventricular sense) was 394 ms and TS maker located near the T wave. On the other hand, time from TS to BV was 850 ms, which was equal to the lower pacing rate limit at 70 bpm. These facts are consistent with the fact

Address for reprints: Takashi Noda, M.D., Division of Cardiology, Department of Internal Medicine, National Cardiovascular Center, 5-7-1 Fujishiro-dai, Suita, Osaka, 565-8565 Japan. Fax: 81-6-6872-7486; e-mail: tnoda@hsp.ncvc.go.jp

Received February 10, 2010; revised March 16, 2010; accepted May 21, 2010.

doi: 10.1111/j.1540-8159.2010.02855.x

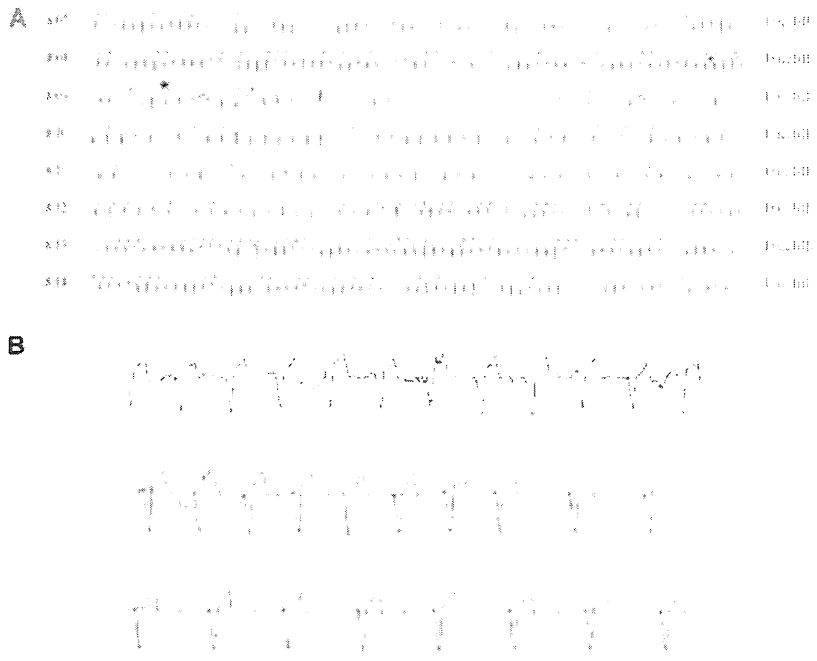

Figure 1. *Abrupt heart rate fallings below the lower pacing rate limit during biventricular pacing. (A) The monitor electrocardiogram showed that abrupt bradycardia at 47 bpm started at the middle of the third line (asterisk) and his heart rate spontaneously recovered to 70 bpm after a while. (B) The enlarged figure of the monitor electrocardiogram showed abrupt bradycardia at 47 bpm.*

of abrupt pacing heart rate fallings at 47 bpm. We changed ventricular blanking period after the pacing from 200 ms to 430 ms, and T-wave oversensing during biventricular pacing disappeared. After adjustment of medical therapy for heart failure, he was discharged. One month later, he complained of multiple presyncopal episodes and T-wave oversensing on intracardiac EGM were observed again. T-wave sensing occurred after the postpacing blanking period. Finally, we adjusted programmed sensitivity from 0.6 mV to 0.9 mV and T-wave oversensing during biventricular pacing has never been observed since then.

Discussion

T-wave oversensing remains an annoying problem in currently available implantable cardioverter defibrillators (ICDs) and CRT-D.[5–7] T-wave oversensing is one of the most common ventricular oversensing malfunction, occurring in 14% of the patients.[8] T-wave oversensing can be divided into three categories: Postpacing, small R wave, and large R wave. The most famous malfunction regarding T-wave oversensing is with small R wave. The ICDs automatically adjust sensitivity in relation to the amplitude of the preceding R wave. At the end of the blanking period after each sensed ventricular event, sensitivity is decreased to a starting value related to the amplitude of the sensed R wave and then decreases with time to a minimum value. This auto-adjusting sensitivity after a sensed ventricular event is useful for detecting ventricular fibrillation (VF) and avoiding T-wave oversensing during sinus rhythm. However, it is sometimes difficult to avoid T-wave oversensing in ICD or CRT-D patients with high T-wave/R-wave ratio. Patients with an ICD or CRT-D whose device shows low-amplitude R waves may require lower minimum sensing thresholds to secure the detection of VF. There is a report regarding Brugada syndrome that the amplitude of T wave decreased and T-wave/R-wave ratio changed spontaneously in the clinical course, which led T-wave oversensing and inappropriate shock.[9] This type of T-wave oversensing is also reported in other heart diseases such as hypertrophic cardiomyopathy and dilated cardiomyopathy.[10] In this situation, we try to manage T-wave oversensing noninvasively by decreasing the ventricular sensitivity, programming longer postventricular sensing refractory periods, and increasing the detection interval count in the tachycardia zone. However, lead revision or the device change to another brand with

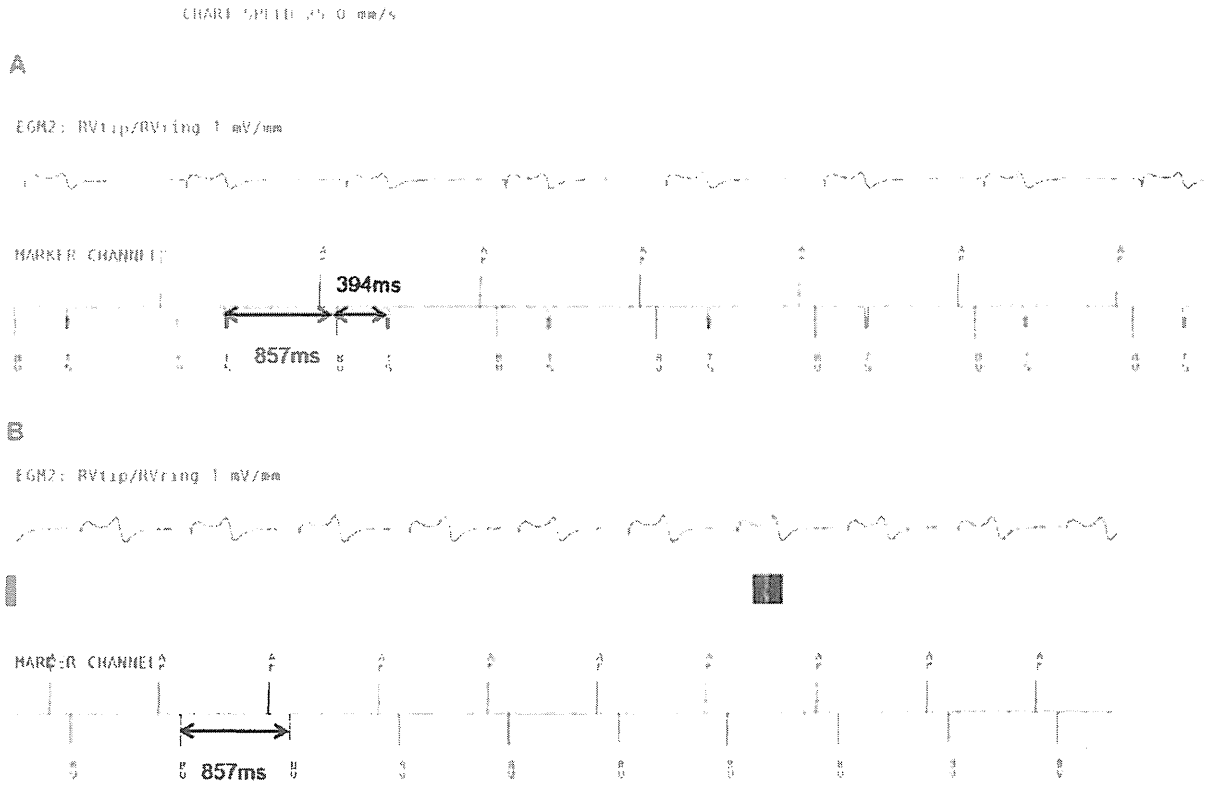

Figure 2. *Intracardiac electrogram during abnormal bradycardia pacing. (A) T-wave oversensing occurred at ventricular sensitivity of 0.6 mV. Time from BV (biventricular pacing spike) to TS (ventricular sense) was 394 ms and TS maker located near the T wave. And time from TS to BV was 850 ms, which was equal to the lower pacing rate limit at 70 bpm. (B) T-wave oversensing disappeared after setting ventricular sensitivity by 0.9 mV.*

more specific filtering to reject T-wave is often necessary.

Postpacing T-wave oversensing can cause inappropriate bradycardia pacing or delivery of antitachycardia pacing at wrong rate.[11] This phenomenon appears only after pacing, so it does not induce inappropriate VF detection. However, it could cause abnormal bradycardia below the lower pacing rate limit, which could be a latent risk for exacerbation of heart failure in CRT patients. Postpacing T-wave oversensing is relatively rare, partly because this problem is not recognized as tachycardia event and is not stored at device EGM. After a pacing pulse, the starting point of the sensitivity threshold is different from that initiated by sensing a spontaneous R wave. A longer ventricular blanking period is required after a ventricular paced event to avoid sensing of T wave of paced beats. In most ICD or CRT-D, ventricular blanking period after bradycardia pace is programmable. In our case, we extended postpacing blanking period in order to avoid postpacing T-wave oversensing. However, maximal extension of postpacing blanking period could not eliminate this problem so that we had to reduce programmed sensitivity. In our case, T-wave oversensing was transient. Although we could not elucidate the cause of this phenomenon, electrolytes balance, body position, and QT interval were considered as the factors of transient manner of this problem. Fortunately, we could detect this event during the hospitalization. However, these events were not recorded on their device and frequently overlooked. Although our patient did not develop syncope, this oversensing might lead to catastrophic syncopal event. Moreover, inappropriate bradycardia pacing could cause heart failure deterioration, especially in a CRT-D patient. We should recognize that T-wave oversensing during biventricular pacing might be overlooked and the only interrogated information is inadequate to evaluate malfunction of CRT device.

Conclusion

Here we experienced abrupt heart rate fallings below the lower pacing rate limit because of postpacing T-wave oversensing in a patient with

CRT-D. Postpacing T-wave oversensing is rare and this problem might be overlooked. As the number of patients with CRT-D will increase more and more in the future, clinicians treating CRT-D patients should be well aware of this malfunction.

References

1. Cleland JG, Daubert JC, Erdmann E, Freemantle N, Gras D, Kappenberger L, Tavazzi L; Cardiac Resynchronization-Heart Failure (CARE-HF) Study Investigators. The effect of cardiac resynchronization on morbidity and mortality in heart failure. N Engl J Med 2005; 352:1539–1549.
2. Bristow MR, Saxon LA, Boehmer J, Krueger S, Kass DA, De Marco T, Carson P, et al. Cardiac-resynchronization therapy with or without an implantable defibrillator in advanced chronic heart failure. N Engl J Med 2004; 350:2140–2150.
3. Mullens W, Grimm RA, Verga T, Dresing T, Starling RC, Wilkoff BL, Tang WH. Insights from a cardiac resynchronization optimization clinic as part of a heart failure disease management program. J Am Coll Cardiol 2009; 53:765–773.
4. Swerdlow CD, Friedman PA. Advanced ICD troubleshooting: Part I. Pacing Clin Electrophysiol 2005; 28:1322–1346.
5. Erven L, Schalij MJ. Troubleshooting implantable cardioverter-defibrillator related problems. Heart 2008; 94:649–660.
6. Koul AK, Keller S, Clancy JF, Lampert R, Batsford WP, Rosenfeld LE. Hypercalemia induced T wave oversensing leading to loss of biventricular pacing and inappropriate ICD shocks. Pacing Clin Electrophysiol 2004; 27:681–683.
7. Gilliam FR. T-wave oversensing in implantable cardiac defibrillators is due to technical failure of device sensing. J Cardiovasc Electrophysiol 2006; 17:553–556.
8. Weretka S, Michaelsen J, Becker R, Karle CA, Voss F, Hilbel T, Osswald BR, et al. Ventricular oversensing: A study of 101 patients implanted with dual chamber defibrillators and two different lead systems. Pacing Clin Electrophysiol 2003; 26(pt 1):65–70.
9. Porres JM, Brugada J, Marco P, Garcia F, Azcarate B. T wave oversensing by a cardioverter defibrillator implanted in a patient with the Brugada syndrome. Pacing Clin Electrophysiol 2004; 27:1563–1565.
10. Washizuka T, Chinushi M, Tagawa M, Kasai H, Watanabe H, Hosaka Y, Yamashita F, et al. Inappropriate discharges by fourth generation implantable cardioverter defibrillators in patients with ventricular arrhythmias. Jpn Circ J 2001; 65:927–930.
11. Manolis AG, Chatzis DG, Kouvelas K, Kyriakides ZS. Partial inhibition of ongoing antitachycardia pacing sequence due to T-wave oversensing. Pacing Clin Electrophysiol 2008; 31:780–781.

Cellular and Molecular Bioengineering, Vol. 5, No. 1, March 2012 *(© 2011)* pp. 113–126
DOI: 10.1007/s12195-011-0219-2

BMES BIOMEDICAL ENGINEERING SOCIETY™ www.bmes.org

Approximation for Cooperative Interactions of a Spatially-Detailed Cardiac Sarcomere Model

TAKUMI WASHIO,[1] JUN-ICHI OKADA,[1] SEIRYO SUGIURA,[2] and TOSHIAKI HISADA[2]

[1]Graduate School of Frontier Sciences, University of Tokyo, 5-1-5, Kashiwanoha, Kashiwa, Chiba 277-0882, Japan; and [2]Graduate School of Frontier Sciences, University of Tokyo, 7-3-1, Hongo, Bunkyo-ku, Tokyo 113-0033, Japan

(Received 25 October 2011; accepted 15 December 2011; published online 28 December 2011)

Associate Editor Andrew D. McCulloch oversaw the review of this article.

Abstract—We developed a novel ordinary differential equation (ODE) model, which produced results that correlated well with the Monte Carlo (MC) simulation when applied to a spatially-detailed model of the cardiac sarcomere. Configuration of the novel ODE model was based on the Ising model of myofilaments, with the "co-operative activation" effect introduced to incorporate nearest-neighbor interactions. First, a set of parameters was estimated using arbitrary Ca transient data to reproduce the combinational probability for the states of three consecutive regulatory units, using single unit probabilities for central and neighboring units in the MC simulation. The parameter set thus obtained enabled the calculation of the state transition of each unit using the ODE model with reference to the neighboring states. The present ODE model not only provided good agreement with the MC simulation results but was also capable of reproducing a wide range of experimental results under both steady-state and dynamic conditions including shortening twitch. The simulation results suggested that the nearest-neighbor interaction is a reasonable approximation of the cooperativity based on end-to-end interactions. Utilizing the modified ODE model resulted in a reduction in computational costs but maintained spatial integrity and co-operative effects, making it a powerful tool in cardiac modeling.

Keywords—Cross-bridge, Monte Carlo simulation, Ordinary differential equation (ODE) model, Contraction force, Sarcomere kinetics.

INTRODUCTION

Mathematical modeling is an indispensable tool in defining the mechanisms of activation and force generation of the cardiac sarcomere. Various mathematical models have been designed to replicate and characterize the cellular processes and activities of the sarcomere and, recently, detailed structure and filament properties have also been taken into account.[2,4,10,16] However, current models have yet to replicate the anomalously high sensitivity of developed force to changes in the free cytosolic calcium (Ca) concentration, observed under both steady-state and dynamic conditions. This aberrant effect is suggested to be brought about by the "co-operative" interactions among intracellular molecules within the sarcomere. One postulated mechanism of "cooperativity" suggests that the strongly-bound cross-bridge releases the steric hindrance of tropomyosin to facilitate the attachment of nearby cross-bridges. A further potential mechanism underlying the "co-operative" interactions is the end-to-end interactions of regulatory troponin/tropomyosin (T/T) units along the thin filament. In either case, the physical arrangement of each molecular component is suggested to be a critical factor.

To reproduce the "co-operative" effects that occur within the sarcomere, most current models utilize the "phenomenological parameter tuning strategy" to normalize the behavior of cross-bridges and to avoid the necessity of determining the state of each regulatory unit and the interactions among them (mean-field approximation). Although this approach enables the use of ordinary differential equations (ODE), has a lower computational cost, and has been reported to provide a fairly good representation of experimental data,[1,9,13,20,21] the models lack a representation of spatial activity within the cell. This limits the predictive ability of the models and hampers the potential for direct comparisons with experimentally obtained data.[18]

Spatially-distributed models have been proposed that are capable of mimicking the physical arrangement of each functional unit within a cell, including the cross-bridges in the thick and thin filaments of the sarcomere.[8,10,19,22] In these models, the transition rates of each unit are dependent on the states of neighboring

Address correspondence to Takumi Washio, Graduate School of Frontier Sciences, University of Tokyo, 5-1-5, Kashiwanoha, Kashiwa, Chiba 277-0882, Japan. Electronic mail: washio@sml.k.u-tokyo.ac.jp

units and/or the cross-bridge strain to reveal any potential "co-operative" mechanisms that occur. Moreover, the models have been found to have excellent reproducibility. However, the inherent and inevitable problem with this type of model is the necessity of using the computationally expensive Monte Carlo (MC) simulation. Although Rice *et al.*[19] reported an analytical solution to their Ising model of myofilaments without MC simulation, its application is limited to the static state with a simple periodic boundary condition. Very recently, Campbell *et al.*[3] proposed a Markov model approach to represent the states of regulatory units, but the computational costs again limited the number of units studied in the model.

Here we propose a novel method for describing the behavior of a spatially detailed co-operative model using ODE in which the regulatory units are distributed along the sarcomere filament. Through modifications to the Ising model produced by Rice *et al.*,[19] we produced an ODE model that is applicable to a wider range of experimental conditions, including accounting for changes in sarcomere length (*SL*). Our modified ODE model was found to correlate well with the MC simulation over a wide range of dynamically changing Ca concentrations. Moreover, our ODE model is capable of recording the information of neighboring units and reproducing the co-operative phenomenon arising from molecular interactions along the sarcomere filaments. Importantly, this novel ODE model is associated with greatly reduced computational costs, thereby enabling its application for large scale models of cardiac physiology.

METHODS

Description of the Model

The sarcomere model used in the present study is illustrated in Fig. 1. The model consists of a pair of thin filaments (AF) and a single thick filament (MF). Myosin heads (MHs) are arranged symmetrically on the thick filament with regular intervals on both sides of the bare-zone (B-zone). The geometry of the model is summarized in Table 1. To introduce *SL* as a factor in the model, we assigned a functional unit to each MH coupled with the opposing segment of thin filament and indexed as "*i*". This process conflicts somewhat with the traditional practices used in sarcomere modeling where the unit is commonly placed on the thin filament. However, because the helical pitch of the myosin filament is close to that of actin (composed of seven monomeric actins) and regulated by a single

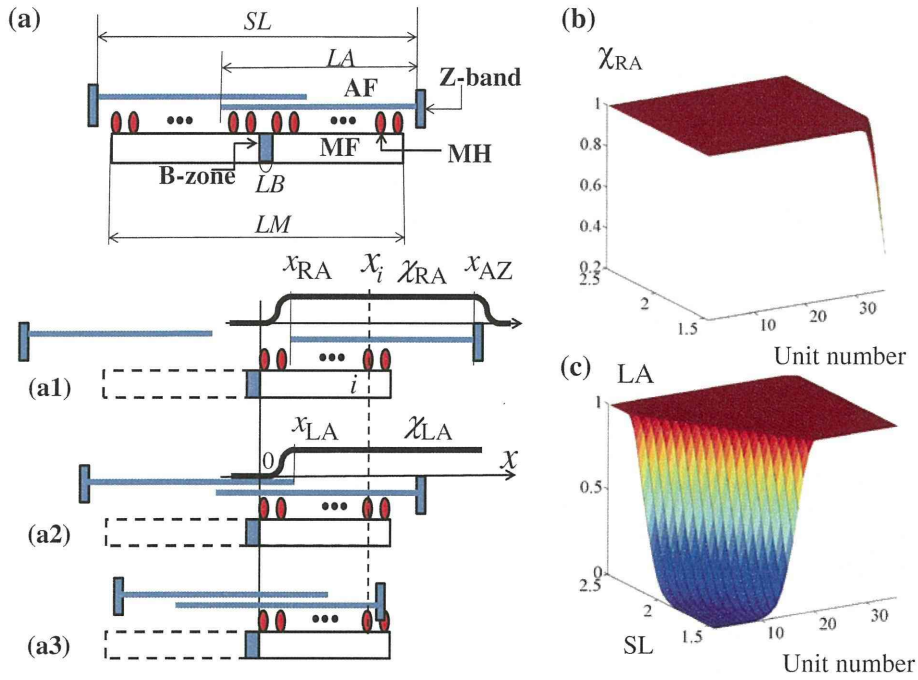

FIGURE 1. Schematic of the sarcomere model (a). (a1) Relative position of filaments in the single overlapping state (*SL* > 2*LA* + *LB*). x_{RA}: position of the end of the right thin filament, x_{AZ}: position of Z-band of the right thin filament, x_i: position of i_{th} MH, both measured from the right-hand edge of the bare zone. (a2) The double overlapping state (*LM* < *SL* < 2*LA* − *LB*). x_{LA}: position of the end of the left thin filament. (a3) State of no overlapping at the MF ends (*SL* < *LM*). MF: thick filament, MH: myosin head, B-zone: bare zone, AF: thin filament, *SL*: sarcomere length LA: thin filament length, LM: thick filament length, LB: bare zone length. Dependence of the lumped parameters $\chi_{RA}(SL, i)$ (b) and $\chi_{LA}(SL, i)$ (c) on *SL* at individual unit (MH_i).

TABLE 1. Model parameters.

Parameter	Value	Units	
Sarcomere geometry			
LA (length of AF)	1.2	μm	*
LM (length of MF)	1.65	μm	*
LB (length of B-zone)	0.1	μm	*
nu (number of MHs)	36	Unitless	*
Transition rates Ca-bound			
K_{on}	80	$\mu M^{-1}\ s^{-1}$	**
K_{off}	80	s^{-1}	**
K'_{on}	80	$\mu M^{-1}\ s^{-1}$	**
K'_{off}	8	s^{-1}	**
Transition rates N–P			**
Q_0	3	Unitless	**
SL_Q	2.2	μm	**
α_Q	1.4	μm^{-1}	**
K_{basic}	10	s^{-1}	**
μ	10	Unitless	**
γ	40	Unitless	**
SL dependence			
a_R	0.1	μm	
a_L	0.1	μm	
Time interval lengths			
DT (for averaging in MC)	2.5	ms	
Δt	2.5	μs	

Parameter values were adopted * from Rice *et al.*,[20] ** from Rice *et al.*[19] with modifications.

troponin/tropomyosin (T/T) complex, we believe this strategy is rational. The model was assumed to be symmetrical, and simulation was performed on half of one sarcomere.

The co-operative four-state Markov model proposed by Rice *et al.*[19] was adopted for the present model whereby the state of each functional unit is characterized by the combination of Ca binding (1: bound, 0: not bound) and cross-bridge formation (P: permitted, N: not permitted; Fig. 2). To introduce the co-operative mechanisms occurring in force generation, the factors γ^n and γ^{-n} were multiplied by the transition rates from N to P and from P to N, respectively, where n (=0, 1 or 2) is the number of nearest-neighboring MHs in the P-state.

In addition, we modified the following rate constants by multiplying the geometrical factors $\chi_{RA}(SL,i)$ and $\chi_{LA}(SL,i)$ (Figs. 1A1, A2, 1B and 1C) to introduce a dependence on the filament overlap determined by *SL*:

$$\begin{aligned}
\bar{K}_{np0}(SL,i) &= \chi_{LA}(SL,i)\chi_{RA}(SL,i)K_{np0},\\
\bar{K}_{np1}(SL,i) &= \chi_{LA}(SL,i)\chi_{RA}(SL,i)K_{np1},\\
\bar{K}_{on}(SL,i) &= \chi_{RA}(SL,i)K_{on},\\
\bar{K}'_{on}(SL,i) &= \chi_{RA}(SL,i)K'_{on}.
\end{aligned} \tag{1}$$

The factors $\chi_{RA}(SL,i)$ and $\chi_{LA}(SL,i)$ were defined for each unit as the function of its position (x_i) and the degree of filament overlap, determined by the positions

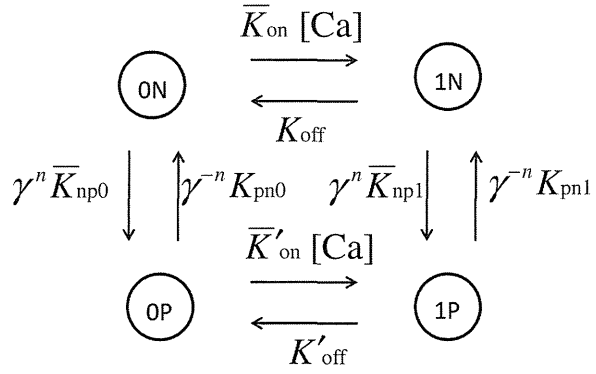

FIGURE 2. The cooperative four-state Markov model. States are coded with the combination of the Ca binding state (0: not bound, 1: bound) and conformation for cross-bridge formation (P: permissive, N: non-permissive). Transitions among the states are governed by the rate constant adjacent to each arrow. To introduce the co-operative behavior for the transition between states P and N, the factors γ^n and γ^{-n} are multiplied by the transition rates from N to P and P to N, respectively, where *n* is the number of neighboring MHs in the P-state. The overlines for transition rates $\bar{K}_{np0}$, $\bar{K}_{np1}$, $\bar{K}_{on}$ and $\bar{K}'_{on}$ indicate that these rates are modified according to the *SL*. [Ca] denotes the free Ca concentration.

of two thin filament ends (the free end (x_{RA}) of the right-hand side filament, the Z-band (x_{AZ}) of the right-hand side filament and the free end (x_{LA}) of the left-hand side filament) (Fig. 1).

$$\begin{aligned}
&x_{AZ} = (SL - LB)/2,\ x_{LA} = LA - x_{AZ} - LB,\\
&x_{RA} = x_{AZ} - LA.
\end{aligned} \tag{2}$$

When there are non-overlapping regions of the two filaments ($SL > 2LA + LB$, Fig. 1A1), only the units where $x_i > x_{RA}$ can form cross-bridges without the modification to the rate constant. For those cross-bridges located in non-overlapping regions ($x_i \le x_{RA}$), the rate constant becomes attenuated as the distance to the MH extends further from the thin filament end:

$$\chi_{RA}(SL,i) = \begin{cases} \exp\left(-(x_{RA} - x_i)^2/a_R^2\right), & x_i \le x_{RA} \\ 1, & x_{RA} < x_i < x_{AZ}, \\ \exp\left(-(x_i - x_{AZ})^2/a_R^2\right), & x_i \ge x_{AZ} \end{cases} \tag{3}$$

where a step function is smoothed at the ends so that χ_{RA} changes continuously with respect to *SL*. The third condition of Eq. (3) becomes effective for determining $\bar{K}_{np0}$ and $\bar{K}_{np1}$ in Eq. (1) when no overlapping state appears at the right ends of MF (Fig. 1A3). The genesis of the ascending limb in the force–length relation in regions of *SL* shorter than the optimal length is a controversial issue. For this model, we assumed that the formation of the cross-bridge was inhibited for

MHs in the double overlap region of the thin filament (Fig. 1A2, $SL < 2LA - LB$):

$$\chi_{LA}(SL, i) = \begin{cases} \exp\left(-(x_{LA} - x_i)^2 / a_L^2\right), & x_i \le x_{LA} \\ 1, & x_i > x_{LA} \end{cases}. \quad (4)$$

The parameters a_R and a_L determine how rapidly the MHs at the borders of overlapping zone lose their capability to form attached bridges as they become distant from the filament ends. The values were adjusted to agree with the experimental force–length relation and are listed in Table 1. Finally, the MHs at the edges of the filament ($i = 1$ and nu) were assumed to always have N-state neighbors on their null side.

Monte Carlo Simulation

The MC simulation was performed according to the following rules. For a given random number $r \in [0, 1]$ generated for each unit (ith MH) at each time interval ($[t, t + \Delta t]$), the state ${}^t\alpha_i$ (either 0N, 1N, 0P, or 1P) at time t transitions to the new state ${}^{t+\Delta t}\alpha_i = T_{\Delta t}({}^t\alpha_i)$ during the time interval $[t, t + \Delta t]$ at all MHs as follows:

$$T_{\Delta t}(0N) = \begin{cases} 1N, & 0 \le r < \Delta t \bar{K}_{on}[Ca] \\ 0P, & \Delta t \bar{K}_{on}[Ca] \le r < \Delta t\left(\bar{K}_{on}[Ca] + \gamma^n \bar{K}_{np0}\right) \\ 0N, & \Delta t\left(\bar{K}_{on}[Ca] + \gamma^n K_{np0}\right) \le r \le 1 \end{cases}$$

$$T_{\Delta t}(1N) = \begin{cases} 0N, & 0 \le r < \Delta t K_{off} \\ 1P, & \Delta t K_{off} \le r < \Delta t\left(K_{off} + \gamma^n \bar{K}_{np1}\right) \\ 1N, & \Delta t\left(K_{off} + \gamma^n \bar{K}_{np1}\right) \le r \le 1 \end{cases}$$

$$T_{\Delta t}(1P) = \begin{cases} 1N, & 0 \le r < \Delta t \gamma^{-n} K_{pn1} \\ 0P, & \Delta t \gamma^{-n} K_{pn1} \le r < \Delta t\left(\gamma^{-n} K_{pn1} + K'_{off}\right) \\ 1P, & \Delta t\left(\gamma^{-n} K_{pn1} + K'_{off}\right) \le r \le 1 \end{cases}$$

$$T_{\Delta t}(0P) = \begin{cases} 1P, & 0 \le r < \Delta t K'_{on}[Ca] \\ 0N, & \Delta t \bar{K}'_{on}[Ca] \le r < \Delta t\left(\bar{K}'_{on}[Ca] + \gamma^{-n} K_{pn0}\right) \\ 0P, & \Delta t\left(\bar{K}'_{on}[Ca] + \gamma^{-n} K_{pn0}\right) \le r \le 1 \end{cases}$$

The time interval Δt was chosen so that none of the values with the coefficient Δt in the third condition of each rule set exceeds 1. The parameter n is the number of nearest-neighboring MHs ($i - 1$th and $i + 1$th MHs) in the P-state at time t.

These transition rate constants were adopted from Rice *et al.*[19] and modified. Some transition rates between the P-state and N-state were calculated with the parameters Q, K_{basic}, μ and γ (Table 1) as follows:

$$K_{np0} = QK_{basic}/\mu,\ K_{np1} = QK_{basic},\ K_{pn0} = K_{basic}\gamma^2,$$
$$K_{pn1} = K_{basic}\gamma^2,\ K'_{on} = K_{on},\ K'_{off} = K_{off}/\mu. \quad (5)$$

To reproduce the SL dependence of $[Ca_{50}]$ on force–pCa relations,[5,14] we introduced the SL dependence of Q. We found that the best results were obtained with the Q value decreasing from $Q_0 = 3$ linearly with inclination $\alpha_Q = 1.4\ \mu m^{-1}$ as the SL becomes shorter from $SL_Q = 2.2\ \mu m$.

$$Q(SL) = \begin{cases} Q_0, & SL \ge SL_Q \\ Q_0 - \alpha_Q(SL_Q - SL), & SL < SL_Q \end{cases} \quad (6)$$

The parameter values are summarized in Table 1.

Approximation by the ODE Model

There are 4^{nu} combinatory states for the model consisting of nu regulatory units. First, we introduced a linear ODE that gives the transitions of probability distribution of these combinatory states for a given Ca transient. This ODE provides a probability distribution that correlated well with the previously described MC simulation. However, the direct solution of this ODE is impractical because of the large number of degrees of freedom (4^{nu} with $nu = 36$ in our case). Therefore, we introduced a reduced ODE to obtain the averaged probability of the four states at each regulatory unit for the solution of the original ODE.

Each of the four states is represented by four integers:

$$0N \leftrightarrow 1,\ 1N \leftrightarrow 2,\ 1P \leftrightarrow 3,\ 0P \leftrightarrow 4 \quad (7)$$

The probability distribution "**P**" can then be represented as a linear combination of the 4^{nu} combinatory states:

$$\mathbf{P} = \sum_{1 \le k_1 \ldots k_{nu} \le 4} P(k_1, \ldots, k_{nu})\ \mathbf{e}(k_1, \ldots, k_{nu}), \quad (8)$$

The following conditions are fulfilled for the coefficients.

$$\sum_{1 \le k_1 \ldots k_{nu} \le 4} P(k_1, \ldots, k_{nu}) = 1,\ \ P(k_1, \ldots, k_{nu}) \ge 0 \quad (9)$$

Here, the basis vector $\mathbf{e}(k_1,\ldots,k_{nu})$ corresponds to the combinatory states of nu units given in Eq. (7), and $P(k_1,\ldots,k_{nu})$ is interpreted as the probability of the total number of units to take this combinatory state.

The vector space representing probability distributions is composed of $m = 4^{nu}$ basis vectors. Because we require $nu = 36$, the dimension m becomes so large that a single vector cannot be stored in the memory of a common computer. However, the transition kinetics of the probability distribution can be expressed by a simple linear ODE as follows.

For any given time t, we define a linear transformation ${}^t\mathbf{A}$ that represents the transition kinetics at time t for the combinatory states by giving its action on the basis vectors:

$$ {}^{t}\mathbf{A}\cdot\mathbf{e}(k_1,\ldots,k_{nu}) = \sum_{1\le i\le nu}\sum_{1\le l\le 4} {}^{t}A_i(\psi(k_{i-1}),\psi(k_{i+1}))_{l,k_i} \times \mathbf{e}(k_1,\ldots,k_{i-1},l,k_{i+1},\ldots,k_{nu}), \quad (10) $$

where ψ indicates the N- or P-state by

$$ \psi(1)=\mathrm{N},\psi(2)=\mathrm{N},\psi(3)=\mathrm{P},\psi(4)=\mathrm{P}. \quad (11) $$

${}^{t}\mathbf{A}_i(\xi,\eta)_{l,k}$ is the (l,k)-component of the 4×4 matrix given by

$$ {}^{t}\mathbf{A}_i(\xi,\eta) = \begin{bmatrix} -\bar{K}_{\mathrm{on}}{}^{t}[\mathrm{Ca}]-\gamma^{n}\bar{K}_{\mathrm{np0}} & K_{\mathrm{off}} & 0 & \gamma^{-n}K_{\mathrm{pn0}} \\ \bar{K}_{\mathrm{on}}{}^{t}[\mathrm{Ca}] & -K_{\mathrm{off}}-\gamma^{n}\bar{K}_{\mathrm{np1}} & \gamma^{-n}K_{\mathrm{pn1}} & 0 \\ 0 & \gamma^{n}\bar{K}_{\mathrm{np1}} & -\gamma^{-n}K_{\mathrm{pn1}}-K'_{\mathrm{off}} & \bar{K}'_{\mathrm{on}}{}^{t}[\mathrm{Ca}] \\ \gamma^{n}\bar{K}_{\mathrm{np0}} & 0 & K'_{\mathrm{off}} & -\gamma^{-n}K_{\mathrm{pn0}}-\bar{K}'_{\mathrm{on}}{}^{t}[\mathrm{Ca}] \end{bmatrix}. \quad (12) $$

Here, n is determined from ξ and η as the sum of the P-state, the transition rates with the overlines are determined from the position of the ith MH (as in Eq. 1), and ${}^{t}[\mathrm{Ca}]$ is the free Ca concentration at time t. From the assumption on the boundary, we can assume that $k_0 = k_{nu+1} = 1$ always holds true in Eq. (10).

It is assumed that the probability distribution ${}^{t}\mathbf{P}$ at time t transposes to the new distribution ${}^{t+\Delta t}\mathbf{P} = T_{\Delta t}({}^{t}\mathbf{P})$ at time $t+\Delta t$. Using the matrix ${}^{t}\mathbf{A}$ defined in Eq. (10), $T_{\Delta t}(\mathbf{e}(k_1,\ldots,k_{nu}))$ (the transition of the specific combinatory state $\mathbf{e}(k_1,\ldots,k_{nu})$) is represented as follows:

$$ T_{\Delta t}(\mathbf{e}(k_1,\ldots,k_{nu})) = \mathbf{e}(k_1,\ldots,k_{nu}) + \Delta t\,{}^{t}\mathbf{A}\cdot \mathbf{e}(k_1,\ldots,k_{nu}) + O(\Delta t^2). \quad (13) $$

The third term from the right-hand side of Eq. (13) is composed of components with coefficients greater than or equal to the second order of Δt. These components correspond to the states that are different from $\mathbf{e}(k_1,\ldots,k_{nu})$ for more than one unit. Thus, by taking the limit $\Delta t \to 0$, the transition kinetics of the probability distribution ${}^{t}\mathbf{P}$ is given by the following linear ODE.

$$ \frac{d^{t}\mathbf{P}}{dt} = {}^{t}\mathbf{A}\cdot{}^{t}\mathbf{P} \quad (14) $$

From Eqs. (10) and (12), it is apparent that the matrix ${}^{t}\mathbf{A}$ has $2nu$ non-zero off-diagonal entries in each column and row when it is represented as the $4^{nu}\times 4^{nu}$ matrix on the basis of $\{\mathbf{e}(k_1,\ldots,k_{nu})\}$. It is also clear that all off-diagonal entries are non-negative and that their sum in each column cancels out exactly with the corresponding diagonal entry. Hence, it can be shown that the properties in Eq. (9) are preserved if the initial distribution satisfies them.

Let $\mathbf{D}_i$ and $\mathbf{D}_i^{\xi,\eta}$ $(1\le i\le nu,\ \xi,\ \eta = \mathrm{P}\text{ or }\mathrm{N})$ be projections from the combinatory probability distribution vector space to the four-dimensional vector space defined by

$$ \mathbf{D}_i\cdot\mathbf{e}(k_1,\ldots,k_i,\ldots,k_{nu}) = \mathbf{e}(k_i), \quad (15) $$

and

$$ \mathbf{D}_i^{\xi,\eta}\cdot\mathbf{e}(k_1,\ldots,k_i,\ldots,k_{nu}) = \begin{cases} \mathbf{e}(k_i) & \text{if } \psi(k_{i-1})=\xi \text{ and } \psi(k_{i+1})=\eta, \\ \mathbf{0} & \text{otherwise,} \end{cases} \quad (16) $$

where $\mathbf{e}(k)$, $(k = 1, 2, 3, 4)$ is the kth unit vector.

Let ${}^{t}[\alpha]_i$ denote the state probability that the i-th MH is in state $\alpha(=\mathrm{0N},\ \mathrm{1N},\ \mathrm{0P},\text{ or }\mathrm{1P})$ and ${}^{t}[\xi,\ \alpha,\ \eta]_i$ denote the combinatorial probability that the ith MH is in state $\alpha(=\mathrm{0N},\ \mathrm{1N},\ \mathrm{0P},\text{ or }\mathrm{1P})$, and the right and left neighbors are in state ξ and $\eta(=\mathrm{N}\text{ or }\mathrm{P})$, respectively, at time t. Thus, with four-dimensional column vectors:

$$ {}^{t}\mathbf{p}_i = [{}^{t}[\mathrm{0N}]_i,{}^{t}[\mathrm{1N}]_i,{}^{t}[\mathrm{1P}]_i,{}^{t}[\mathrm{0P}]_i]^{T} = \mathbf{D}_i\cdot{}^{t}\mathbf{P} \quad (17) $$

and

$$ {}^{t}\mathbf{p}_i^{\xi,\eta} = [{}^{t}[\xi,\mathrm{0N},\eta]_i,{}^{t}[\xi,\mathrm{1N},\eta]_i,{}^{t}[\xi,\mathrm{1P},\eta]_i,\ {}^{t}[\xi,\mathrm{0P},\eta]_i]^{T} = \mathbf{D}_i^{\xi,\eta}\cdot\ {}^{t}\mathbf{P},\ \ \xi,\eta=\mathrm{N}\text{ or }\mathrm{P}, \quad (18) $$

The transition kinetics of the ith MH can be described as follows:

$$ \frac{d^{t}\mathbf{p}_i}{dt} = \sum_{\xi,\eta=\mathrm{N,P}} {}^{t}\mathbf{A}_i(\xi,\eta)\cdot{}^{t}\mathbf{p}_i^{\xi,\eta}, i=1,\ldots,nu. \quad (19) $$

Understandably, this equation cannot be solved as an ODE because it requires the combinatory probability ${}^{t}[\xi,\ \alpha,\ \eta]_i$ at the right-hand side, whereas the variables of the ODE are the state probabilities ${}^{t}[\alpha]_i$. Accordingly, the vector ${}^{t}\mathbf{p}_i^{\xi,\eta}$ and its component $({}^{t}[\xi,\ \alpha,\ \eta]_i)$ require approximation using information available from the MC simulation. For this purpose, we focus on the correlation between the combinatory probability ${}^{t}[\xi,\ \alpha,\ \eta]_i$ and the state probabilities ${}^{s}[\beta]_j(\beta = \mathrm{0N},$